(2)

NAVAL POSTGRADUATE SCHOOL
Monterey, California

THESIS

ASSESSMENT OF THE EFFECTS OF REFRACTIVE CONDITIONS ON ELECTRONIC WARFARE IN CENTRAL AMERICA

by

Mauricio Gaviria Maldonado

September, 1990

Thesis Advisor: Kenneth L. Davidson

REPORT DOCUMENTATION PAGE

1a REPORT SECURITY CLASSIFICATION UNCLASSIFIED	1b RESTRICTIVE MARKINGS
2a SECURITY CLASSIFICATION AUTHORITY	3 DISTRIBUTION/AVAILABILITY OF REPORT Approved for public release; distribution is unlimited.
2b DECLASSIFICATION/DOWNGRADING SCHEDULE	
4 PERFORMING ORGANIZATION REPORT NUMBER(S)	5 MONITORING ORGANIZATION REPORT NUMBER(S)
6a NAME OF PERFORMING ORGANIZATION Naval Postgraduate School 6b OFFICE SYMBOL (*If applicable*) 55	7a NAME OF MONITORING ORGANIZATION Naval Postgraduate School
6c ADDRESS (*City, State, and ZIP Code*) Monterey, CA 93943-5000	7b ADDRESS (*City, State, and ZIP Code*) Monterey, CA 93943-5000
8a NAME OF FUNDING/SPONSORING ORGANIZATION 8b OFFICE SYMBOL (*If applicable*)	9 PROCUREMENT INSTRUMENT IDENTIFICATION NUMBER
8c ADDRESS (*City, State, and ZIP Code*)	10 SOURCE OF FUNDING NUMBERS Program Element No / Project No / Task No / Work Unit Accession Number

11 TITLE (*Include Security Classification*)
ASSESSMENT OF THE EFFECTS OF REFRACTIVE CONDITIONS ON ELECTRONIC WARFARE IN CENTRAL AMERICA

12 PERSONAL AUTHOR(S) MAURICIO GAVIRIA MALDONADO

13a TYPE OF REPORT	13b TIME COVERED	14 DATE OF REPORT (*year, month, day*)	15 PAGE COUNT
Master's Thesis	From To	September 1990	74

16 SUPPLEMENTARY NOTATION
The views expressed in this thesis are those of the author and do not reflect the official policy or position of the Department of Defense or the U.S. Government

17 COSATI CODES			18 SUBJECT TERMS (*continue on reverse if necessary and identify by block number*)
FIELD	GROUP	SUBGROUP	Refractive Conditions, Proagation, Central America, Radar, Microwave.

19 ABSTRACT (*continue on reverse if necessary and identify by block number*)

This thesis presents a study of the atmospheric refractivity conditions in the oceanic area around Central America and a description of the possible propagation effects on surveillance systems. The basic principles of atmospheric refraction are presented along with the techniques used to determine the occurrence of atmospheric ducts and to characterize the type of refractive profiles occuring at a station. Radiosonde data collected by coastal stations in the area were used to establish refractive conditions.

20 DISTRIBUTION/AVAILABILITY OF ABSTRACT	21 ABSTRACT SECURITY CLASSIFICATION	
☒ UNCLASSIFIED/UNLIMITED ☐ SAME AS REPORT ☐ DTIC USERS	UNCLASSIFIED	
22a NAME OF RESPONSIBLE INDIVIDUAL K. L. Davidson	22b TELEPHONE (*Include Area code*) (408)-646-2309	22c OFFICE SYMBOL MR

DD FORM 1473, 84 MAR 83 APR edition may be used until exhausted
All other editions are obsolete

Approved for public release; distribution is unlimited.

Assessment of the effects of Refractive Conditions
on Electronic Warfare in Central America

by

Mauricio Gaviria Maldonado
Lieutenant, Colombian Navy

Submitted in partial fulfillment
of the requirements for the degree of

MASTER OF SCIENCE IN SYSTEMS ENGINEERING
(Electronic Warfare)

from the

NAVAL POSTGRADUATE SCHOOL
September 1990

Author: _____
Mauricio Gaviria Maldonado

Approved by: _____
Kenneth. L. Davidson, Thesis Advisor

_____
Scott H. Hershey, Second Reader

_____
Joseph Stenberg, Chairman
Electronic Warfare Academic Group

ABSTRACT

This thesis presents a study of the atmospheric refractivity conditions in the oceanic area around Central America and a description of the possible propagation effects on surveillance systems. The basic principles of atmospheric refraction are presented along with the techniques used to determine the occurrence of atmospheric ducts and to characterize the type of refractive profiles occurring at a station. Radiosonde data collected by coastal stations in the area were used to establish refractive conditions.

TABLE OF CONTENTS

LIST OF FIGURES

I. INTRODUCTION

A. PURPOSE

Modern warfare tactics rely heavily on the performance of radar and communications systems, both ground based and mobile. Although new technology has made significant hardware improvements that have extended range detection (power increases, antenna design, digital signal processing, e.g.), the atmospheric effects on these systems still play an important role in their performance.

The study of refraction effects has been concentrated in those areas where the U.S. military has spent a lot of time, such as the Persian Gulf, the California coast and the Mediterranean sea, or areas that present obvious abnormal refraction conditions. The purpose of this work is to establish overall refractive conditions, determine the availability of data for the region and evaluate the role of the near surface refraction effects on the performance of surveillance and ESM (Electronic Support Measures) systems for the Central America region.

B. BACKGROUND

Many studies have been performed in different areas of the world which have resulted in well documented anomalous propagation, especially in the Mediterranean, Indian and Northern Pacific oceans. However, an in depth study

of refractive conditions does not appear to exist for the Central America's two ocean influence region.

A general meteorological description of the area exists and is given by the Forecasters Handbook for Central America and Adjacent Waters (Naval Environmental Prediction Facility, Technical Report TR 89-09, 1989). However, the description has not considered the refraction phenomena of the region and their effects on radio-wave propagation in depth.

Military operations in open ocean and coastal environments depend on accurate atmospheric data to estimate systems performance and have to rely on the existence of sufficient knowledge of the environment. Unfortunately, data has been and continues to be insufficient to meet most planning as well as operational needs. The purpose of this thesis is to provide atmospheric information and analysis of the Central America region to aid military commands.

There are computer based models that have been in use for several years to assess the effects of the various atmospheric conditions on the performance of specific systems. One model is EREPS (Engineers's Refractive Effects Prediction System), similar to IREPS (Integrated Refractive Effects Prediction System), which is used by the U.S. Navy for operational propagation assessment. Such microcomputers models provide a convenient way to investigate the effects of particular atmospheric conditions on the performance of systems.

II. ATMOSPHERIC REFRACTION

A. WAVE PROPAGATION

The propagation of the electromagnetic energy is strongly affected by the atmosphere in several ways: refraction, absorption and noise generation [Ref. 1] as well as by other phenomena. The latter includes scintillation and fading, due to atmospheric inhomogeneities, and turbulence and optical interference, due to multi-path propagation.

There are at least four well differentiated propagation categories: ground wave, line of sight, ionospheric and scatter propagation. For low frequency ranges (up to perhaps 1500 KHz) ground wave propagation is the main propagation mechanism. The ground wave is radiation directly affected by the surface of the earth at the interface. In general, it is vertically polarized and very stable over time. For higher frequencies, the ionospheric propagation becomes important up to a critical frequency near the end of the HF range. Solar induced ionization of the upper atmosphere is the dominant factor in the propagation. There are large daily and long term variations in the virtual height and strength of the reflecting layers which affect the frequencies that can propagate and the absorption levels between any given points. For frequencies above HF the propagation mechanism is mainly space wave or line of sight (LOS) propagation. Here, the main loss

factor in the propagation is due to the spherical spreading of the wavefront that decreases the signal strength as the inverse of the square of the distance.

The fourth category is scatter propagation that occurs when inhomogeneities (in the troposphere) or ions (in the ionosphere) scatter and reradiate the incident energy in all directions. A small amount of this energy will eventually reach the receiver located beyond the LOS path. This mechanism can lead to reliable, stable microwave links as long as enough power is used to overcome the losses.

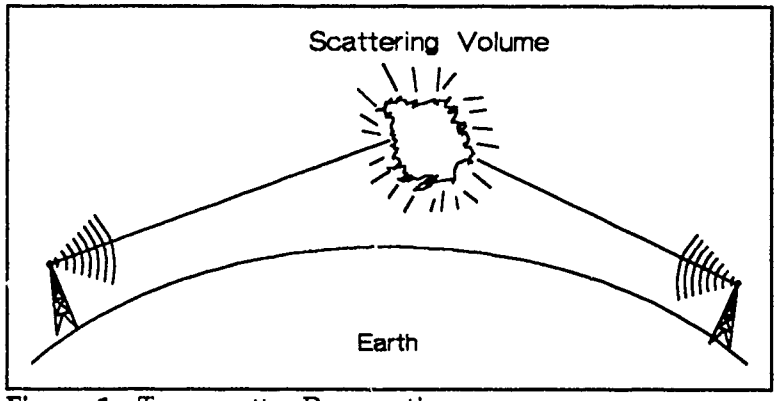

Figure 1. Troposcatter Propagation.

This thesis will focus on microwave and, hence, space wave propagation. When microwaves propagate through the atmosphere they are affected mainly by the lower atmosphere, troposphere, between sea level and approximately 15,000 meters. This is the part of the atmosphere that presents the strongest changes in pressure, temperature and humidity that determine the refractivity. The most severe effect, due to refractive variation, occurs when a layer of air with a

negative refractivity gradient bends the rays back toward the earth trapping the energy inside a duct.

B. ATMOSPHERIC REFRACTIVITY

Deviations from rectilinear wave propagation are determined by the variations in the index of refraction of the atmosphere. The main variation of the latter is in the vertical direction and is due to the pressure, humidity, and temperature changing with height. Refraction occurs because of speed variations along the path of the wave that are described by the index of refraction.

The radio and radar waves propagate through the lower atmosphere at a speed, v, lower than the free-space speed as determined by the electromagnetic properties of the medium:

$$v = \frac{c}{\sqrt{\mu * k}}$$

where:

c = speed of light

μ = magnetic permeability

k = specific inductive capacity

The ratio of free-space speed to the actual phase propagation speed in the medium is defined as index of refraction, n, with a typical value for air of 1.0003 at sea level.

The Equation for atmospheric refractivity is obtained from the Debye's theory of the dielectric constant of gases [Ref. 3]:

$$\frac{\varepsilon-1}{\varepsilon+2}=\frac{4\pi\,\text{Å}}{3\,M}*\rho\left[\alpha+\frac{1}{3}\frac{\mu^2}{KT}*\left(\frac{1}{1+i\omega\tau}\right)\right]$$

where:

- ε = Dielectric constant = n^2
- Å = Avogadro's number
- K = Boltzman's constant
- M = Molecular weight
- μ = Electric dipole moment
- τ = Relaxation time
- ω = Frequency of exiting field
- α = Polarization
- ρ = Density
- T = Temperature

At frequencies below approximately 60 GHz., the relative response time of the molecules with respect to the frequency makes the product $\omega*\tau$ very small with respect to 1. Since $\varepsilon = n^2$ and from the equation of state $\rho=\frac{P}{RT}$ [Ref. 2], the expression then becomes:

$$(n-1)=2\pi\frac{\text{Å}}{M}*\frac{P}{RT}*\left[\alpha+\frac{1}{3}\frac{\mu^2}{KT}\right]$$

The pressure P is the sum of the water vapor pressure, e, and the dry air pressure, P_d. The molecular weight, M, is also the sum of the dry air, M_d, and

water vapor M_w, components. With contribution of these two components identified separately, the index of refraction for moist air is:

$$(n-1)=\frac{C_1}{M_d}*\frac{(P-e)}{T}\alpha_d+\frac{C_1\ e}{M_w\ T}*(\alpha_w+C_2\frac{1}{T})$$

where:

$$C_1=\frac{2\pi\text{Å}}{R} \qquad C_2=\frac{\mu_w^{\ 2}}{3K}$$

Assigning values to the constants, leads to the refractivity being conveniently expressed with the following equation [Ref. 3]:

$$N = (1-n)*10^6 = \frac{77.6*P}{T}+\frac{3.73*10^5*e}{T^2}$$

where:

N = Refractivity
n = Index of refraction
P = Pressure, mbar
T = Absoiute temperature, Kelvin
e = Partial pressure of water vapor, mbar

The physical composition of the air through the entire troposphere is almost constant as far as the oxygen, nitrogen and other gases are concerned. The refractivity depends, then, mainly on the temperature and water vapor contained in the air. The contribution of the water-vapor term to the refractivity is relatively small for cold air because then the saturated vapor pressure is small. But for warm air the term becomes important and the water-vapor content has a strong influence on the value of N.

There are no special absorption effects up to 60 GHz., where the oxygen molecule shows its first resonance [Ref. 4], well above the frequencies of most surveillance radars.

The water content of the air decreases rapidly with height, as does pressure, while the temperature decreases slowly to the tropopause where it stabilizes. These changes in the meteorological variables lead to refractivity decreasing with height, under normal conditions (Standard Atmosphere), at a rate of 39.37 N units per Km. A decrease of N with height means that as height increases, the wave propagates faster, closer to the free space speed, causing the rays to bend downward following Snell's law as shown in Figure 2.

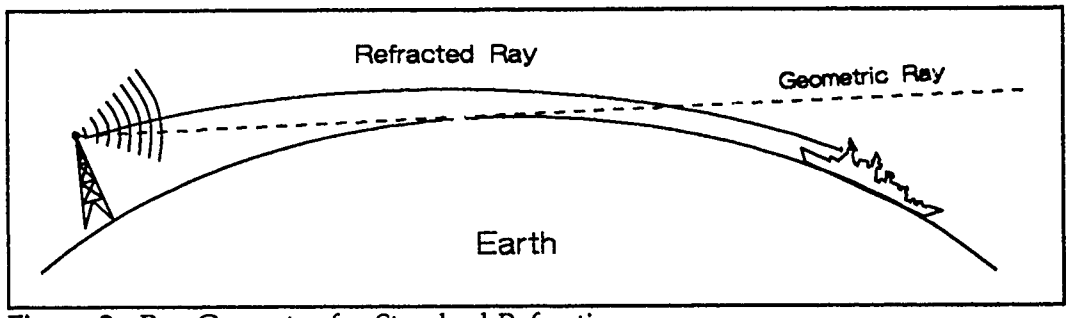

Figure 2. Ray Geometry for Standard Refraction.

To use radar for tactical purposes, the exact knowledge of the path followed by the waves and their speed are needed to compute position of the target from the timing and angle measured. Since radar systems base their position

calculations on U.S. or ICAN "Standard Atmosphere" at any given time, when the atmospheric conditions differ, the calculated position of target may be wrong and it becomes necessary to include refraction effects in the interpretation of radar products.

The abnormal (anomalous) propagation of electromagnetic waves is called subrefraction, super-refraction or trapping, according to the extent and direction of the deviation of the rays from standard.

C. TYPES OF REFRACTIVITY PROFILES

1. Standard Atmosphere

The International Civil Aviation Organization (ICAO) has defined a standard sounding for the atmosphere at non-tropical latitudes that begins with a surface (sea-level) temperature of 15 Celsius. Clearly, it is not applicable to tropical latitudes where the sea-level temperature is usually 26 Celsius and, therefore, a warmer and, importantly, a more humid Marine Atmospheric Boundary Layer (MABL) is expected. Jordan (1958) [Ref. 5] has formulated a Mean Tropical Atmospheric Sounding that is useful for calculating a base profile of refractivity at tropical latitudes (see Figure 3).

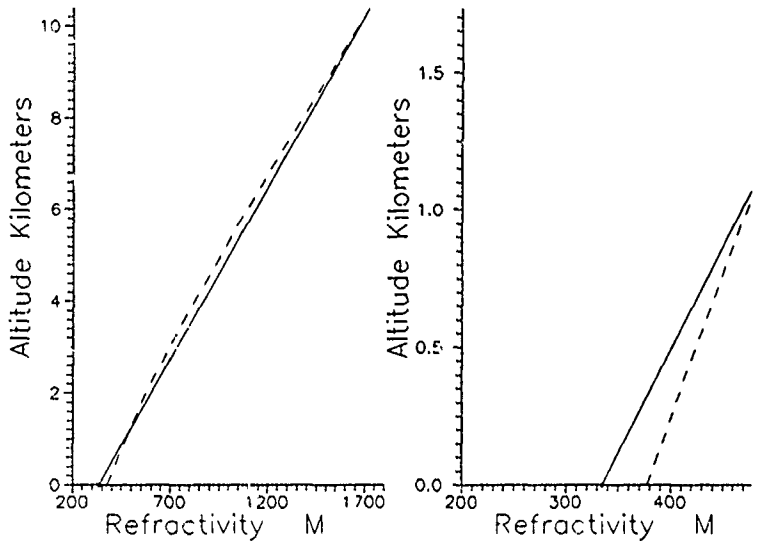

Figure 3. Modified Refractivity Profile, Mean Tropical Sounding and Low Altitude Detail.

The low altitude detail in Figure 3 shows the refractive profile in the lower atmosphere for both the ICAN standard atmosphere and that of the mean tropical sounding by Jordan [Ref. 5]. The refractivity gradient at the low altitude is greater for the tropical atmosphere which would lead to greater radio/radar horizon.

The distance, d, to the radio horizon is related to the refractivity gradient by:

$$d = \sqrt{2 * k * a_e * h_t}$$

where, h_t, is the transmitter height and k is the ratio of the effective earth's radius, a_e, to the actual radius of the earth, a :

$$a_e = \frac{1}{\left[\frac{1}{a} + \frac{dn}{dZ}\right]}$$

The ratio, k, was calculated for the first kilometer in the mean tropical sounding as $k = 1.722$ where for the ICAN standard atmosphere its value is 1.333. The radio/radar horizon is proportional to $k^{1/2}$ for a given transmitter height. Therefore, on the average, the Jordan tropical sounding has 14% larger radio horizon.

2. Superrefractivity and Trapping

The atmospheric conditions in which superrefractivity and trapping of microwave energy occurs always involve stratification of the atmosphere into layers of different index of refraction. Trapping layers and resulting ducts can be surface based or elevated. Elevated and surface based trapping layers can be detected by radiosonde temperature, pressure and humidity measurements and by direct measurement of the refractive profile with an airborne refractometer.

Superrefractive layers are formed when there is a layer in which the temperature increases with height (the temperature decreases with altitude with a lapse rate of 9.8 Kelvin per Km in a well mixed atmosphere) and/or the water vapor sharply decreases with height. Superrefractive layers become trapping layers when the refractivity gradient causes the propagating wave to bend downward with a radius of curvature smaller than the radius of curvature of the

earth. The energy is reflected at the surface again, (surface based duct), or refracted back by the base layer, (elevated duct), trapping it inside the duct as depicted in Figure 4.

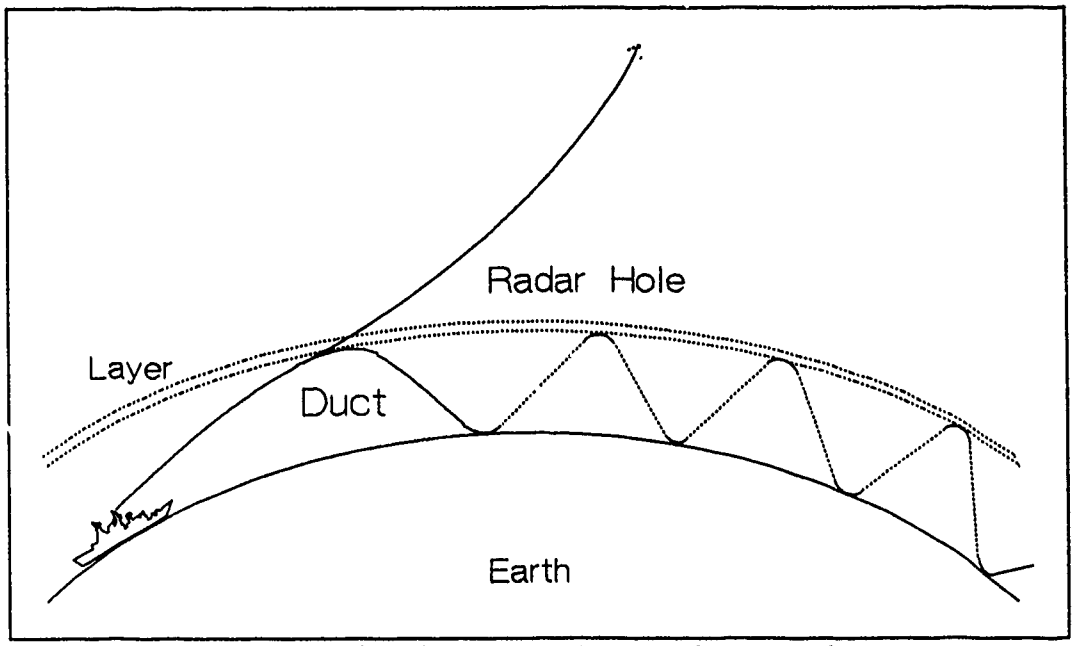

Figure 4. Propagation of Radar Energy in a Surface Based Duct.

Figure 5 illustrates how the different duct types relate to the various refractive profiles.

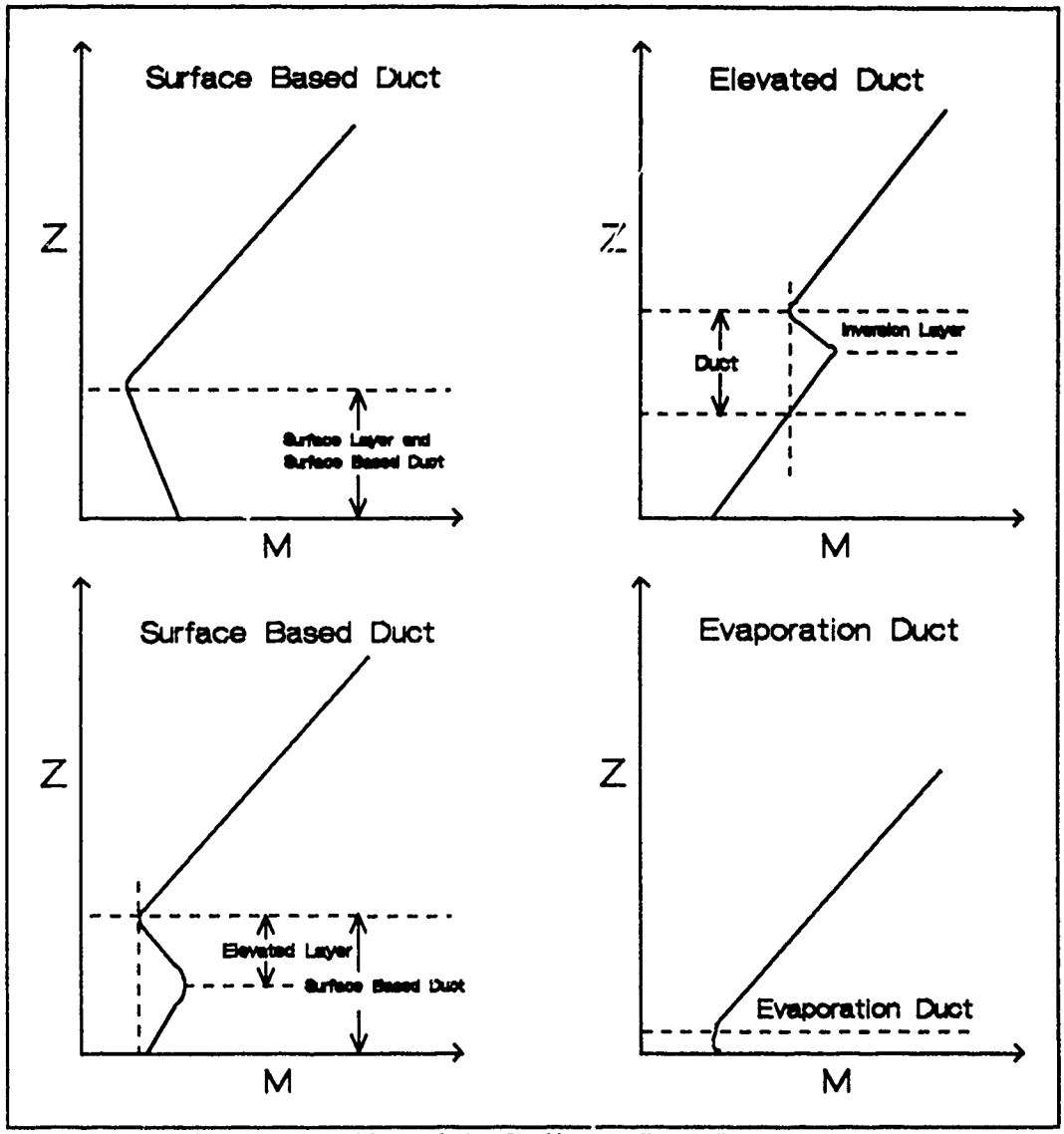

Figure 5. Refractive Profiles of the Different Duct Types.

The evaporation duct is due to an abrupt change in relative humidity at the water-air interface, from 100 % to approximately 85 % in the first few meters. The

evaporation duct is almost always present over water. Its thickness varies as a result of the daily temperature changes and intensity of the surface wind. The evaporation duct height can be computed from bulk meteorological measurements (sea surface temperature, air temperature and wind) by using semi-empirical models like the model described by Paulus [Ref. 6]. For a given duct thickness, d, the minimum frequency, F_{min}, that can propagate within the duct is given by [Ref. 4]:

$$F_{min} = \frac{C}{2.5 * \left(-\frac{\partial n}{\partial z}\right)^{\frac{1}{2}} * d^{\frac{3}{2}}}$$

The minimum frequency propagated in the surface based duct as a function of the duct thickness can be seen in Figure 6.

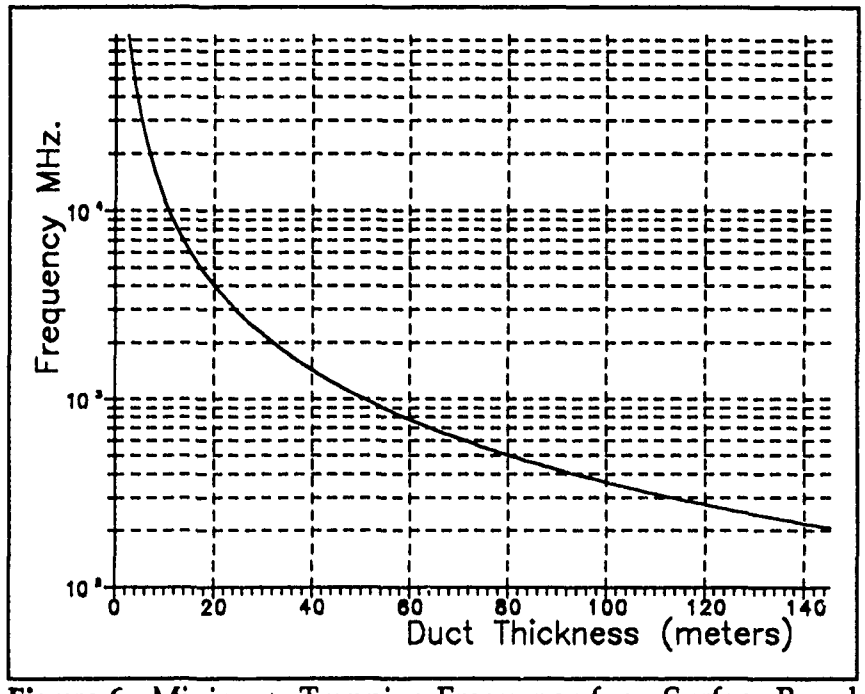

Figure 6. Minimum Trapping Frequency for a Surface Based Duct.

D. METEOROLOGICAL PHENOMENA LEADING TO TRAPPING

Several meteorological conditions modify the distribution of temperature and water vapor in the lower atmosphere. Variations in temperature, pressure, or both, determine as described before, the atmospheric refractive gradient. Air flow associated with the motion of air masses, radiation, subsidence and land-sea winds, define the vertical temperature and moisture profile of the atmosphere.

a. Radiation

Radiative cooling of the surface during clear nights is a very common cause of temperature inversion leading to superrefractive conditions over

land. At sea, the ocean acts as a massive heat reservoir so its surface temperature remains nearly constant and the effect is diminished.

b. Subsidence

Subsidence, the slow, large scale sinking of the air, brings dry air from aloft and raises the temperature of the air by adiabatic compression. This creates inversion layers that are common on large tropical and subtropical ocean areas. Subsidence occurs within subtropical high pressure systems.

c. Land-sea winds

The difference in temperature and humidities between the land, heated by the sun, and the adjacent sea surface usually causes the warmer, dry air over land to rise and subside over the adjacent cooler and more moist marine air. The colder moist air from the sea will replace the raising air as depicted in Figure 7. The warm, dry air will form the upper boundary of an inversion layer in which ducting can occur.

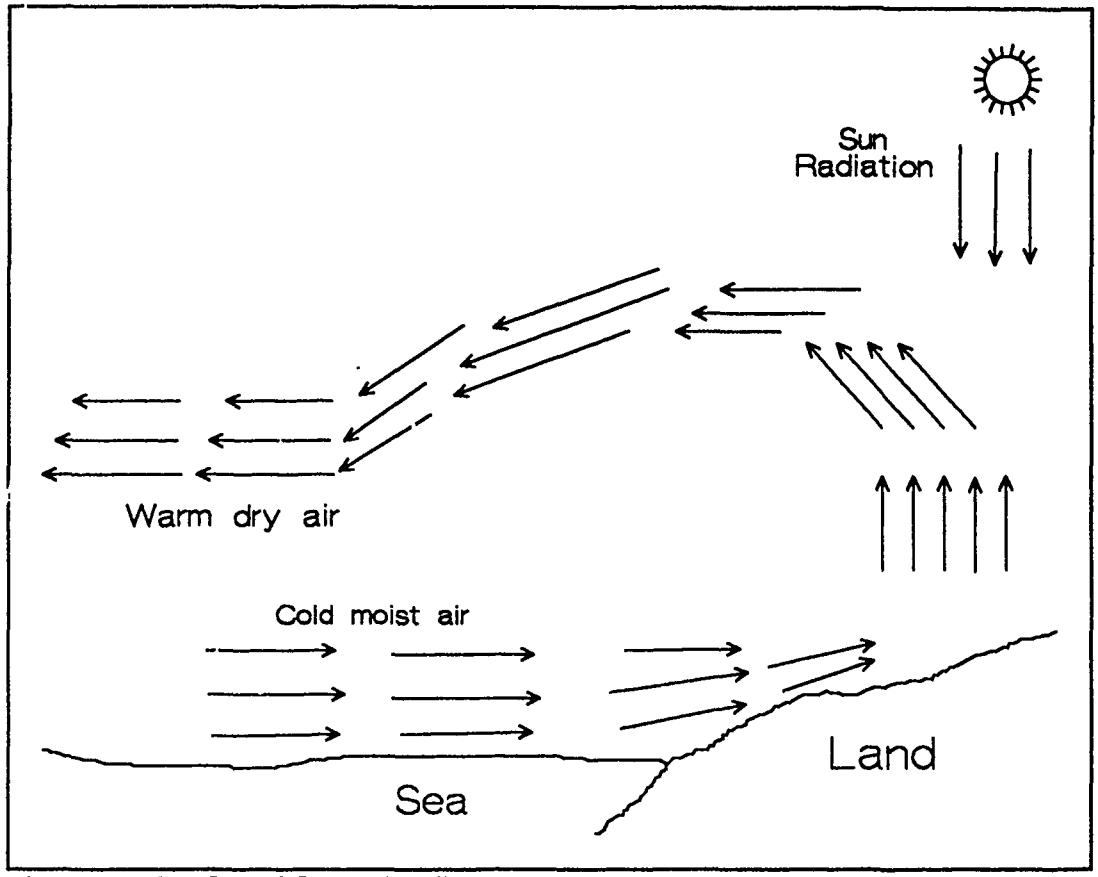

Figure 7. Sea-Wind Inversion Layer.

III. CENTRAL AMERICA CLIMATOLOGY

A. CLIMATOLOGY

The meteorology of Central America is significantly influenced by the Intertropical Convergence Zone (ITCZ) that lies on the pacific side most of the year [Ref. 7]. The large scale air flow along the ITCZ is the product of the northeasterly trade winds meeting the southeasterly trade winds. Since they are air masses of different origin, their temperatures and water vapor content are quite different making the ITCZ a zone of very high cloudiness and precipitation that can be seen all year around in the satellite imagery. Rainfall occurs primarily between June and September and by December with drier periods in between.

The general air flow direction along the ITCZ is west-to-east during most of the year. It is deviated by the Andean ranges at the western coast of South America, which have heights up to 5000 meters. The Caribbean side is mostly affected by the flow of trade winds that flow in harmony with the general Caribbean regime. Here the dominant phenomena are the tropical disturbances. Sea surface temperatures are high in both Pacific and Caribbean areas, with small diurnal and annual changes [Ref. 8], which in turn cause very constant surface air temperatures.

B. SYNOPTIC DESCRIPTION

The Pacific and Caribbean sides of Central America are subject to different regimes. The Pacific presents a general surface air flow following the ITCZ parallel to the equator that ends at the western coast of South America where is deviated by the high Andes mountains. The Caribbean is farther north and is less affected by the ITCZ.

Local phenomena, such as like sea-breeze and land-sea winds are known to cause strong inversion layers in coastal areas. The breezes are frequent and strong enough to dominate the general circulation. The complete synoptic description of the area can be found in the Forecasters Handbook for Central America and Adjacent Waters [Ref. 7].

IV. DATA ANALYSIS AND RESULTS

A. RADIOSONDE DATA

1. Geographical Distribution of Data

For the purpose of this study, we have considered data taken during 1988 and 1989 by the stations shown in Figure 8. These are listed in Table 1.

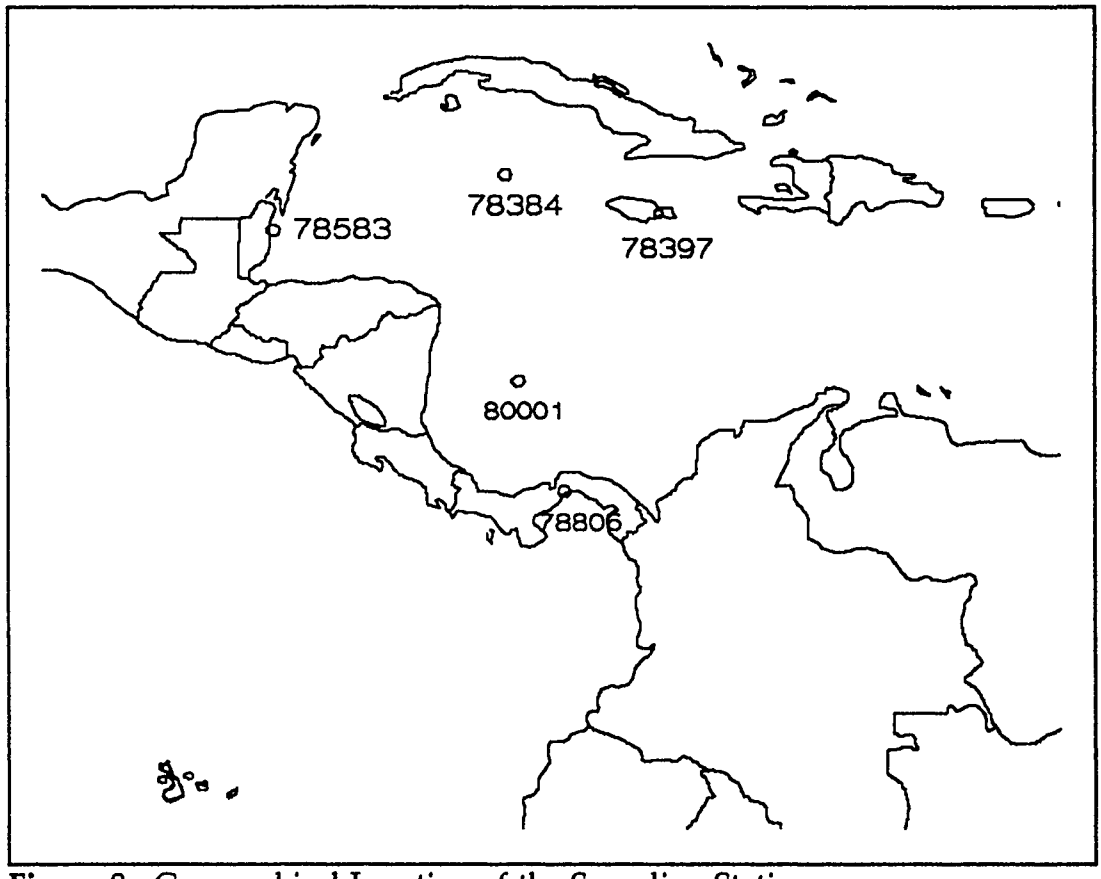

Figure 8. Geographical Location of the Sounding Stations.

Table 1

Stations Used in the Analysis

Station		Lat.	Long.	Elev.
78384	Roberts Field, Gran Cayman Island	18-19N	81-20W	3 m
78397	Kingston, Jamaica	18-04N	76-50W	1 m
78583	Belize International Airport, Belize	17-36N	88-18W	5 m
78806	Howard A.F.B., Panama	8-58N	79-35W	66 m
80001	San Andres Island, Colombia	12-34N	81-41W	2 m

There is only one station located on the Pacific side of Central America (station 78806 in Howard A.F.B., Panama) in the area of this study. Two of the five stations located in the Caribbean are in the Greater Antilles (stations 78384, 78397 in Jamaica and Gran Cayman), one is in an open ocean island (station 80001, San Andres) and one is a coastal station in Belize (station 78583).

2. Distribution of Data Over Time

Stations are supposed to launch radiosondes twice a day (stations 78806, 78583, 78397, 78384) and daily in the case of station 80001 [Ref. 9]. Due to different circumstances they generally do not. The resultant distribution of soundings is presented according to stations in Table 2.

Table 2

Distribution of Radiosonde Data Over Time, Average Monthly Launchings

Station	Name	Jan	Feb	Mar	Apr	Mar	Jun	Jul	Aug	Sep	Oct	Nov	Dic
78384	Gran Cayman Island	117	67	102	98	106	98	93	55	80	114	104	104
[illegible]97	Kingston, Jamaica	127	79	121	92	102	103	93	83	88	103	93	88
78583	Belize	93	61	33	19	48	39	58	61	47	58	33	65
78806	Howard A.F.B., Panama	76	54	90	57	31	67	95	103	63	19	70	51
80001	San Andres Island	51	24	29	30	42	47	30	47	51	47	29	15

B. ANALYSIS OF REFRACTIVE CONDITIONS

1. Procedure of Analysis

The Fleet Numerical Oceanography Center, Monterey, CA, provided significant and mandatory level radiosonde data on 9-track tape for 1988 and 1989. The tape files were read and transferred to a PC-type microcomputer for processing. Pressure, temperature and dew-point depression from significant levels were used to calculate refractivity and height for display as a refractivity profile and to compute the refractivity gradient to identify anomalous conditions.

Since ducts occur at various altitudes, with a broad strength range, it is difficult to appropriately describe with statistical measures the refractive profile. Therefore, each refractive profile in which ducting was detected was displayed and visually evaluated with the purpose of stating a typical ducting profile for each station. EREPS was used to graphically show the effects of these profiles on a typical radar system performance.

The ray tracing subprogram of EREPS (RAYS) was used to visualize effects of the typical refractive anomalies detected in the soundings. The propagation model (PROP) [Ref. 10] was used to assess the performance of typical systems under the ducting conditions detected. Finally, the evaporation duct climatology from EREPS is used to visualize the expected effect of the evaporation duct in surveillance radar and ESM systems.

2. Formulas and Algorithms

Formulae used in the programs to identify and plot ducts are presented here and the general procedure followed to determine the occurrence of ducts in the soundings.

Modified Refractivity is calculated from pressure, temperature, partial pressure of water vapor and height with the following equation:

$$M = \frac{77.6 * P}{Ta} + \frac{3.73 * 10^5 * e}{Ta^2} + \frac{h}{6.371}$$

where:

P = Pressure in millibars
Ta = Temperature in Kelvin
e = Partial pressure of water vapor in millibars
h = Height in meters

Partial water vapor pressure was calculated from the saturated vapor pressure at a the dew point temperature. The saturated water vapor pressure for a given temperature is calculated using Lowe's polynomial [Ref. 11]:

$$Es = A_6 * T^6 + A_5 * T^5 + A_4 * T^4 + A_3 * T^3 + A_2 * T^2 + A * T + A_0$$

where:

A_0 = 6.107799961000000
A = 0.443651852100000
A_2 = 0.014289458050000
A_3 = 0.000265064847100
A_4 = 0.000003031240396
A_5 = $2.0340809481 * 10^{-8}$
A_6 = $6.136820928999999 * 10^{-11}$
T = Temperature in Celsius

The Height is calculated from the initial launch altitude and pressure for the first level, and from the preceding level for the successive heights using the relationship for geopotential height [Ref. 12], as expressed in the following equation:

$$h = h_0 + 14.63*(Vt_0+Vt_1)*Log(\frac{P_0}{P_1})$$

where:

h_0 = Initial Height, meters
Vt_0 = Virtual Temperature at Initial Height, Kelvin
P_0 = Pressure at Initial Height , mbar
Vt_1 = Virtual Temperature at Actual Height, Kelvin
P_1 = Pressure at Actual Height , mbar

Virtual temperature is computed from the temperature, pressure and water vapor pressure with the equation:

$$Vt = Ta + \frac{(0.3794017*Ta*e)}{(P-e)}$$

where:

Ta = Absolute temperature (Kelvin)
P = Pressure
e = Vapor pressure.

The trapping layers are identified by computing the refractive gradient $\partial M/dZ$ and plotting the refractive profile, modified refractivity, M, versus height,

for the data sets that have negative gradient to visually evaluate the resulting trapping layers.

3. Results by Stations

a. San Andres Island, Station 80001

A total of 442 soundings where processed for this station. Trapping layers were classified as being surface based or not, and if not, as being above or below 700 mb. Trapping layers were found in 156 soundings, and are distributed as follows according to occurrence being at the surface or, if not, as being above or below 700 mb :

Year	1988	1989	Total
Soundings	161	281	442
Surface based trapping layers	15	16	31
Elevated trapping layers (total)	41	84	125
Elevated trapping layers above 700 mb.	10	20	30
Total	56	100	156

The refractive profiles that showed trapping layers were visually evaluated and it was found that trapping layers were stratified much like the profile in Figure 11. Many profiles showed more than one trapping layer and therefore have multiple ducts. Only the lower trapping layer per sounding was used for the

above statistics. The trapping layer height was about 2000 meters and below. The thickness and intensity of trapping layers were less than or equal to the profiles shown. The local launch time for this station is 06:30 (12:00 UT). Therefore the observations are representative of a stable, non mixed MABL in which stratification is enhanced.

Soundings revealing trapping layers had many data errors. Nineteen of the 156 layers identified by the program were due to errors in the data. These were identified visually by checking the suspect part of the data for robustness. Surface based trapping layers were found to occur in 7 % of the soundings. Because surface trapping layers could have been caused by erroneous launch level values, they were checked closely. The total duct occurrence found is 31 %, after excluding the errors. For this station, Ortenburguer and Lawson [Ref. 13] has found an occurrence of surface based ducts of 20 % and an occurrence of elevated ducts of 35%.

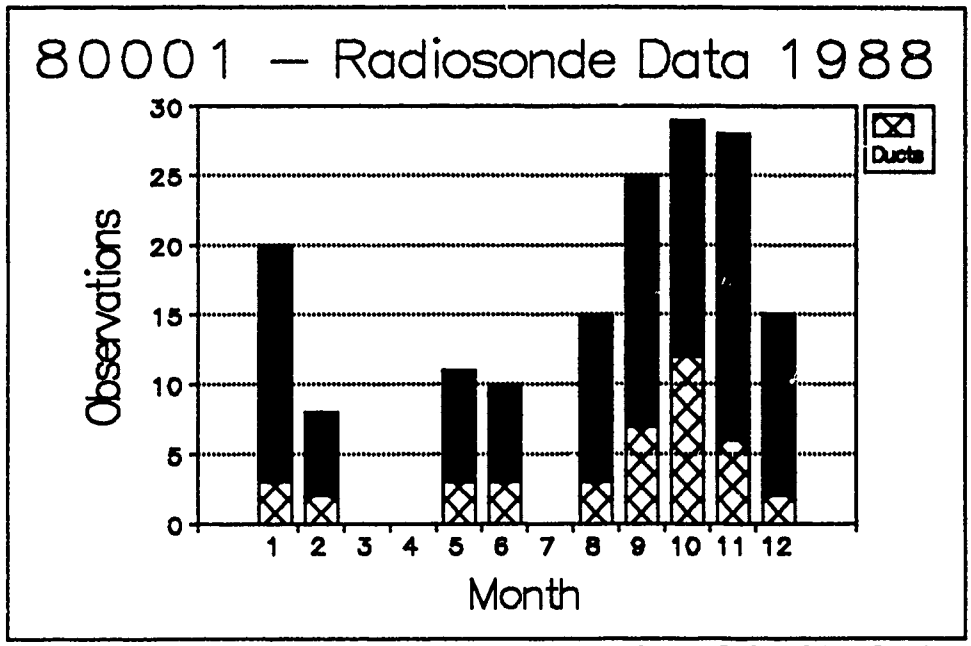

Figure 9. Radiosonde Data, 1988, San Andres, Colombia, Station 80001.

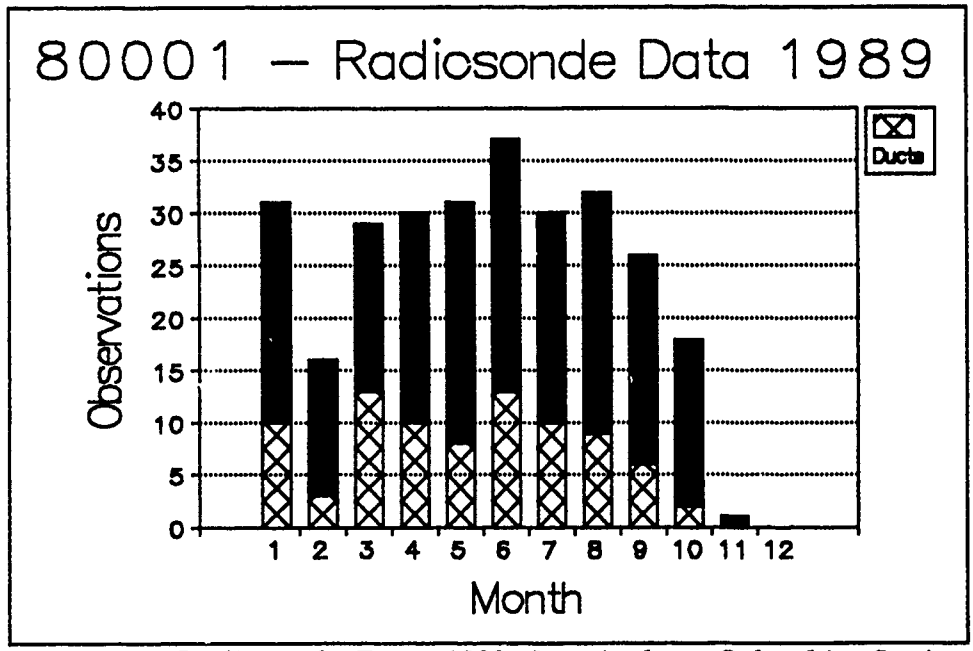

Figure 10. Radiosonde Data, 1989, San Andres, Colombia, Station 80001.

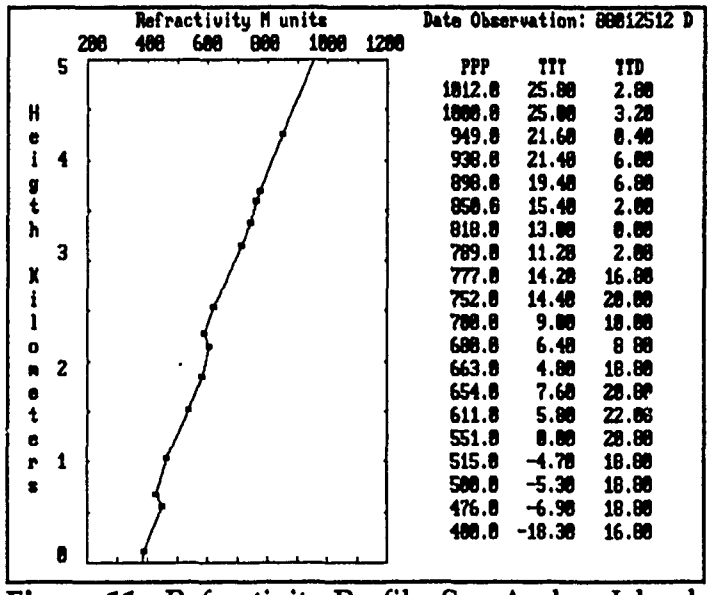

Figure 11. Refractivity Profile, San Andres Island, Station 80001, 25 Jan 1988.

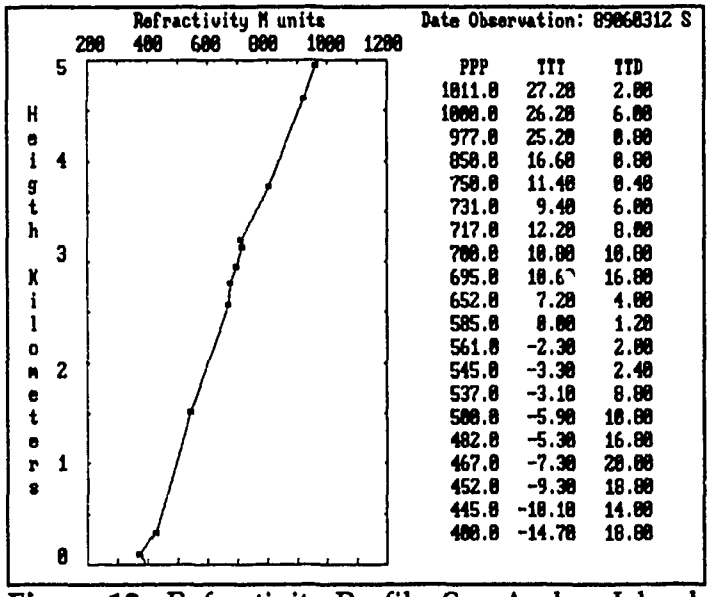

Figure 12. Refractivity Profile, San Andres Island, Station 80001, 3 Jun. 1989.

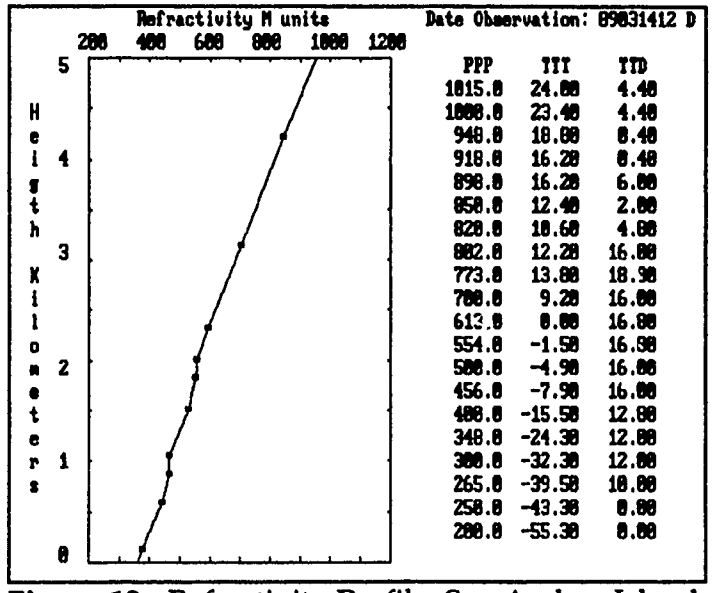

Figure 13. Refractivity Profile, San Andres Island, Station 80001, 14 Mar. 1989.

b. Howard A.F.B., Panama, Station 78806

For this station 766 soundings where processed, trapping layers were found in 266 soundings distributed as follows:

Year	1988	1989	Total
Soundings	417	359	776
Surface based trapping layers	45	45	90
Elevated trapping layers (total)	107	69	176
Elevated trapping layers above 700 mb.	25	16	41
Total	152	114	266

The soundings that showed trapping layers were visually evaluated. The occurrence of trapping layers was observed centered at around 2500 meters and the associated ducts tend to be strong and thick as seen in the profile of Figure 16. The strength of the duct refers to the M difference across the duct while thickness refers to the vertical separation of the duct top and base. Many refractive profiles contain more than one trapping layer and associated duct. Local launch times are 06:41 and 18:41 (12:00 UT and 00:00 UT). Data from these times could have greater ducting occurrence than mid-day time data due to lesser convection generally occurring before sunrise and after sunset.

Visual inspection of the first 5000 meters in the profiles that showed trapping layers, revealed fifteen data sets in error of the total 266 soundings with trapping layers found by the program. This reduces the duct occurrence found from 34.7 % to 32.3 %. The surface based inversion layer occurred in 11.6 % of the soundings. As was described above, a surface based inversion layer could arise from erroneous surface values. This possibility was checked very closely for this case because the percent occurrence of surface based trapping layers was above 10%. For this station, Ortenburguer and Lawson [Ref. 13] has found an occurrence of surface based ducts of 5 % and an occurrence of elevated ducts of 29 %.

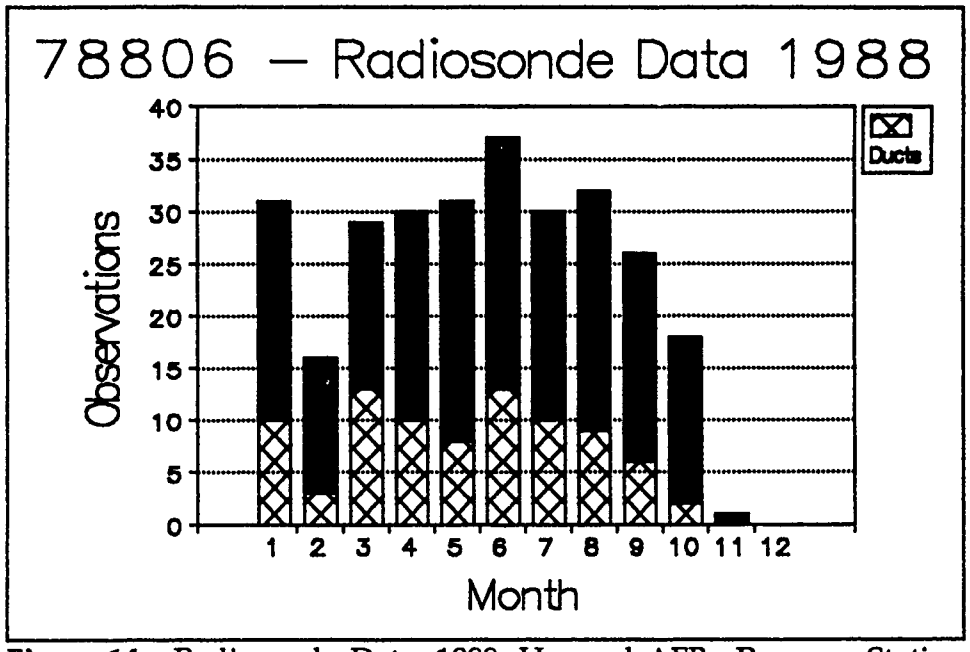

Figure 14. Radiosonde Data, 1988, Howard AFB., Panama, Station 78806.

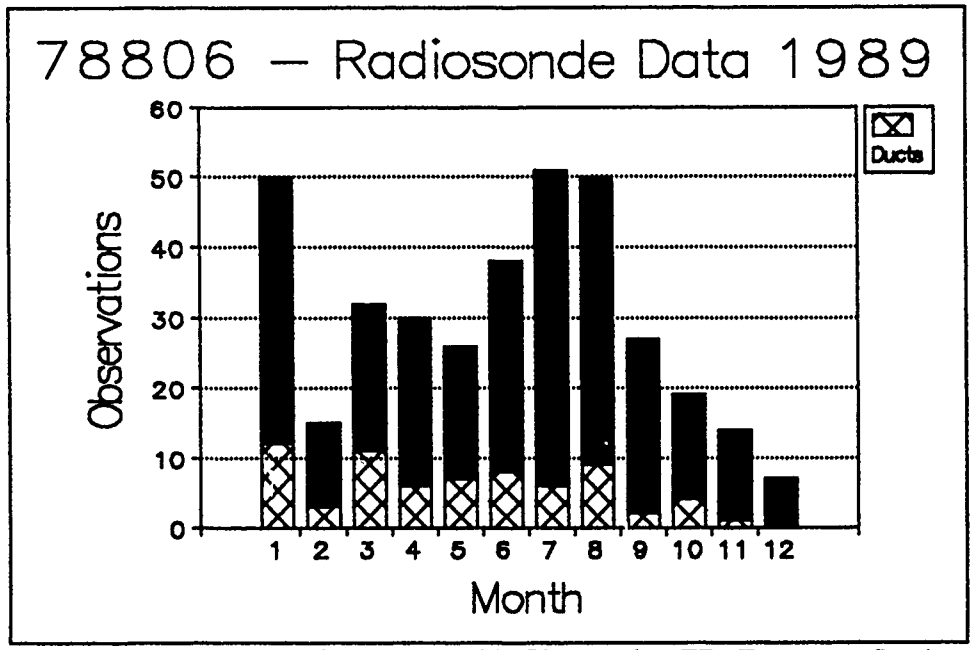

Figure 15. Radiosonde Data, 1989, Howard AFB, Panama, Station 78806.

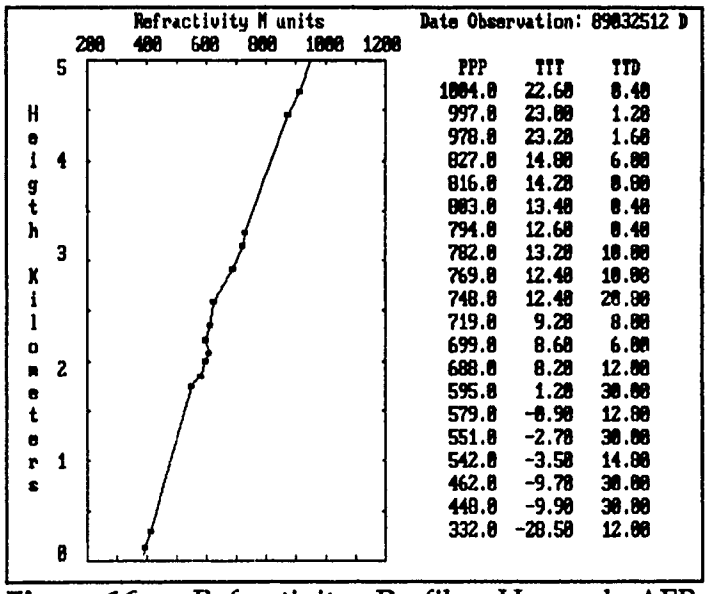

Figure 16. Refractivity Profile, Howard AFB, Panama, Station 80001, 25 Mar. 1989.

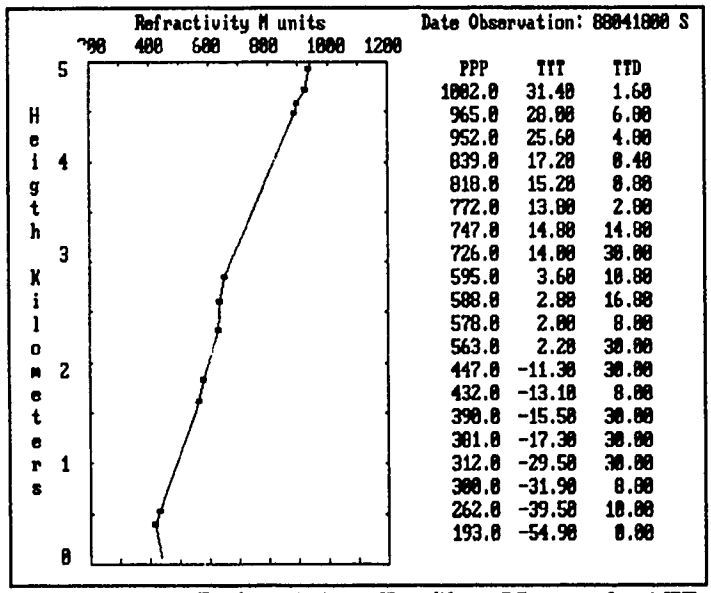

Figure 17. Refractivity Profile, Howard AFB, Panama, Station 78806, 13 Apr. 1988.

c. *Belize Airport, Belize, Station 78583*

A total of 615 soundings where processed for this station. Trapping layers and associated ducts were found in 188 soundings and are distributed as follows:

Year	1988	1989	Total
Soundings	397	218	615
Surface based trapping layers	10	7	17
Elevated trapping layers (total)	108	63	171
Elevated trapping layers 700 mb.	36	13	49
Total	118	70	188

The elevated trapping layers occurred consistently at an altitude of about 1700 to 2000 meters. There where few multiple duct occurrences and the few surface based ducts where not very strong. Figure 20 and Figure 21 show typical M profiles. The inversion layer is stronger and thicker in the 12:00 UT sounding.

Two errors were detected in the data of the soundings found with ducts. The percentage of trapping layer occurrence was 30.2 %. Surface based inversion layers occurred in 2.8 % of the soundings. This station is not included in the work by Ortenburguer and Lawson [Ref. 13].

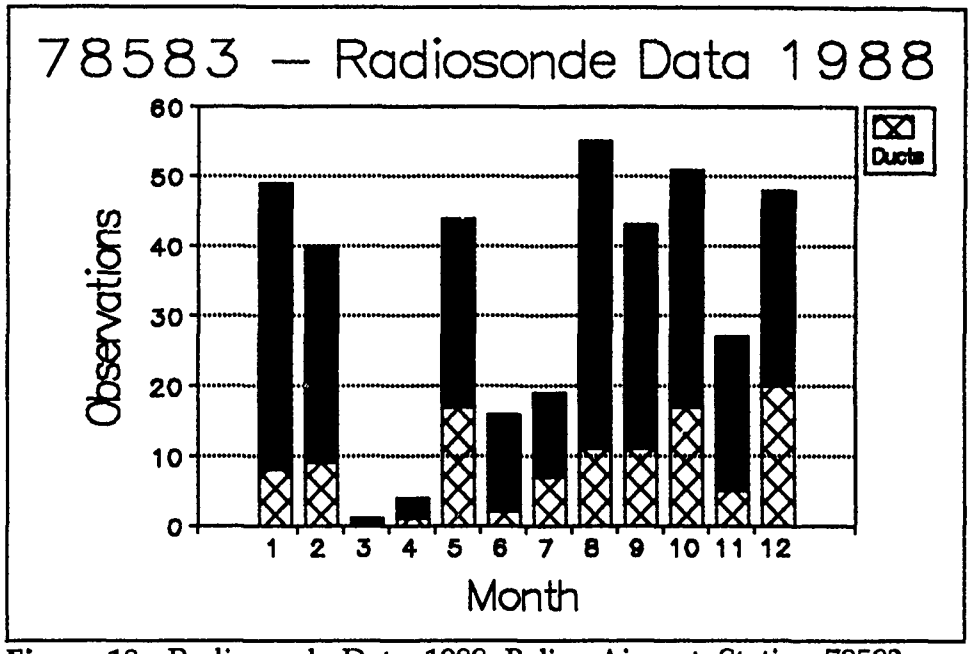

Figure 18. Radiosonde Data, 1988, Belize Airport, Station 78583.

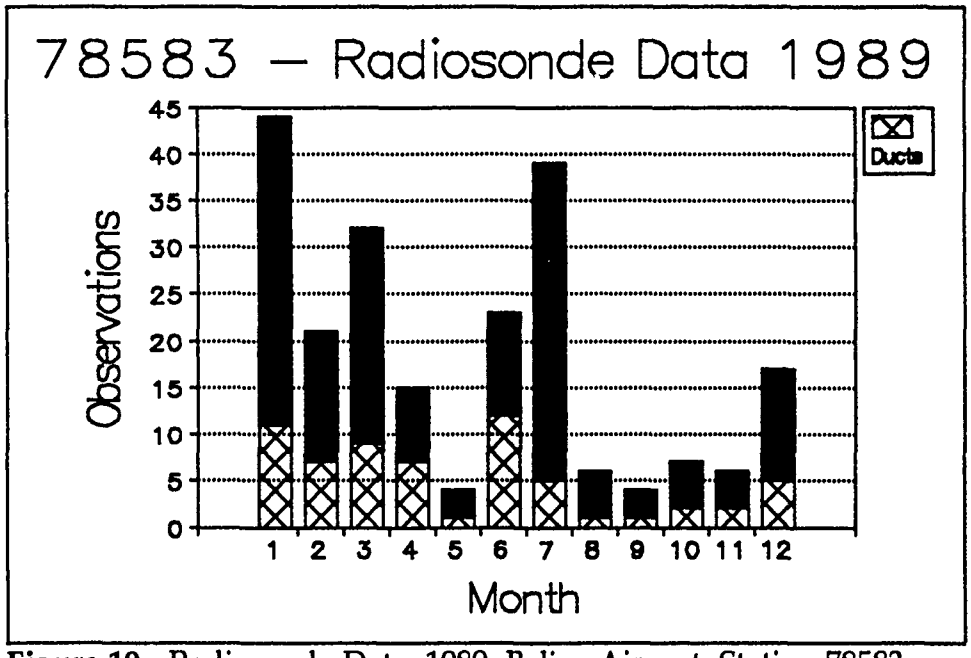

Figure 19. Radiosonde Data, 1989, Belize Airport, Station 78583.

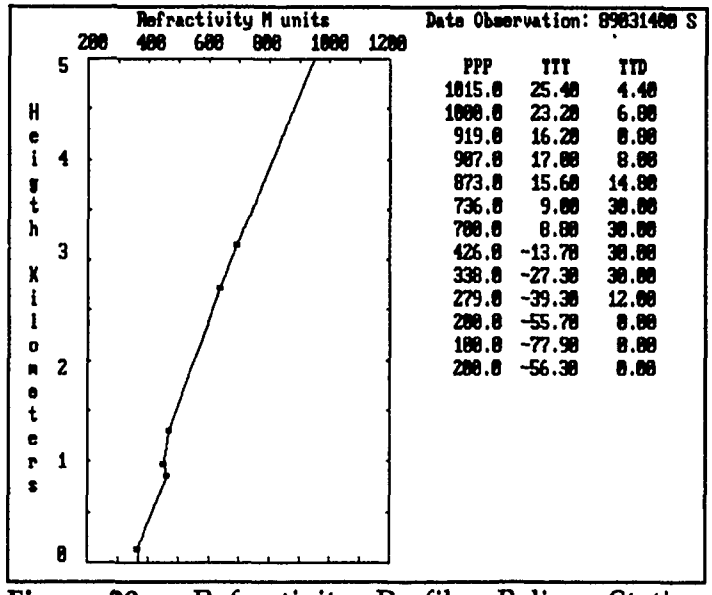

Figure 20. Refractivity Profile, Belize, Station 78583, 14 Mar. 1989.

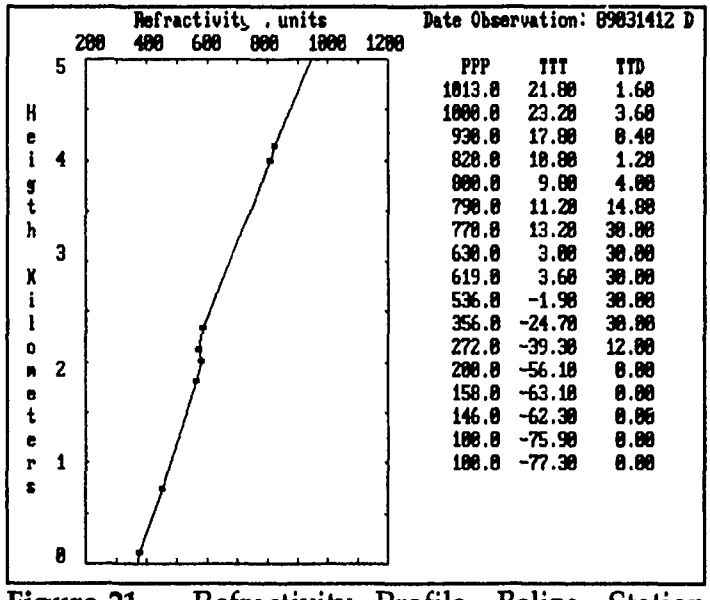

Figure 21. Refractivity Profile, Belize, Station 78583, 14 Mar. 1989.

d. Kingston, Jamaica, Station 78397

A total of 1182 soundings were processed for this station. Trapping layers and associated ducts were found in 248 soundings and are distributed as follows:

Year	1988	1989	Total
Soundings	659	523	1182
Surface based trapping layers	24	16	40
Elevated trapping layers (total)	123	85	208
Elevated trapping layers above 700 mb.	25	27	52
Total	147	101	248

Visual evaluation of the 147 refractive profiles that showed trapping layers revealed nineteen erroneous data sets. The trapping layer is located generally at 2000 to 2500 meters. Most ducts are neither strong nor thick. The profiles shown in Figure 24 and Figure 25 are representative of the strongest trapping layers seen. The frequency of occurrence of trapping layers was 19.4 %. Surface based trapping layers occurred in 3.4 % of the soundings. For this station, Ortenburguer and Lawson [Ref. 13] has found an occurrence of surface based ducts of 20 % and an occurrence of elevated ducts of 33 %.

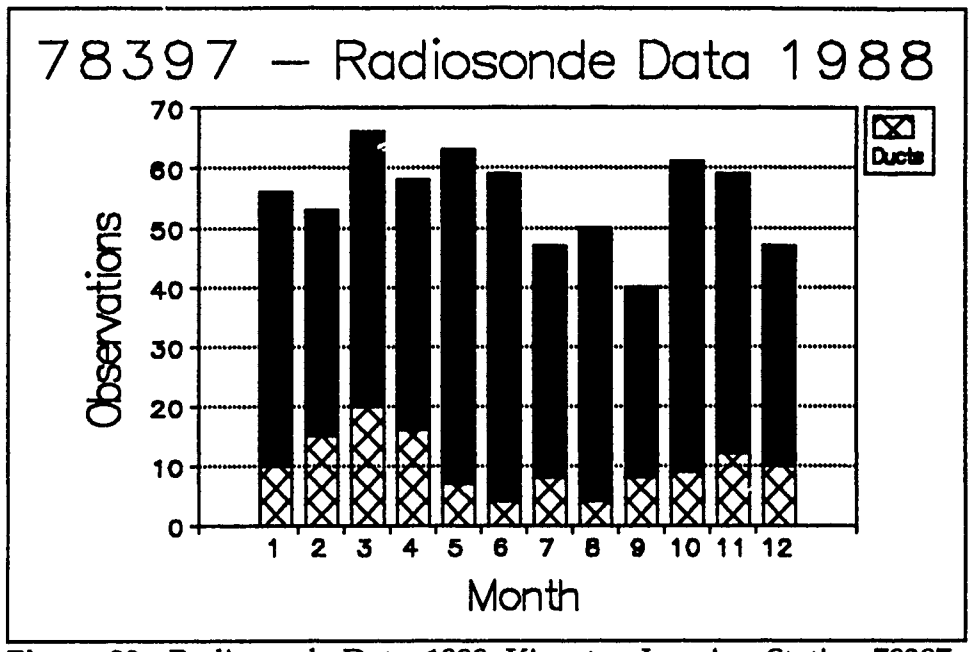

Figure 22. Radiosonde Data, 1988, Kingston Jamaica, Station 78397.

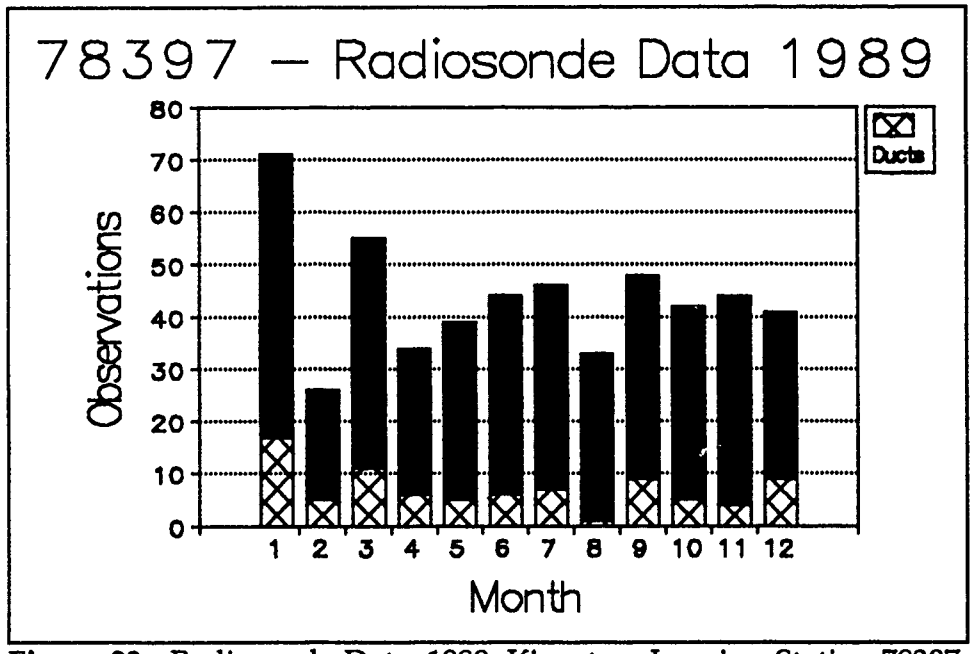

Figure 23. Radiosonde Data, 1989, Kingston, Jamaica, Station 78397.

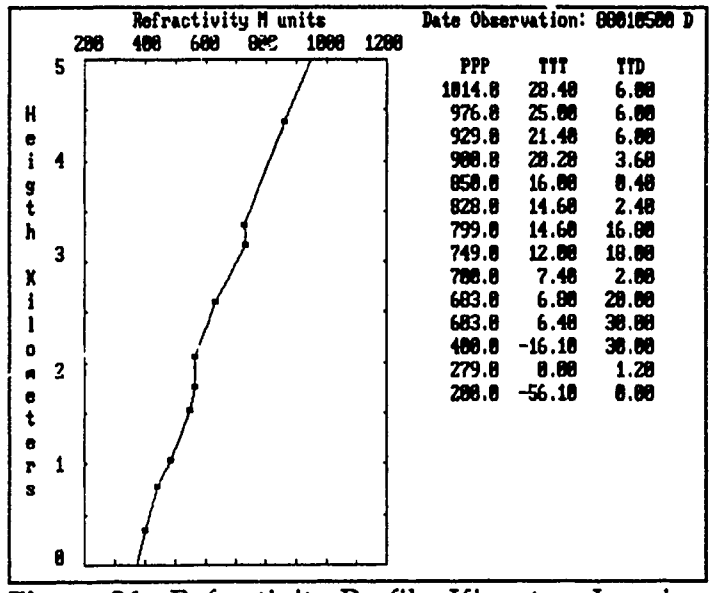

Figure 24. Refractivity Profile, Kingston, Jamaica, Station 78397, 5 Jan. 1988.

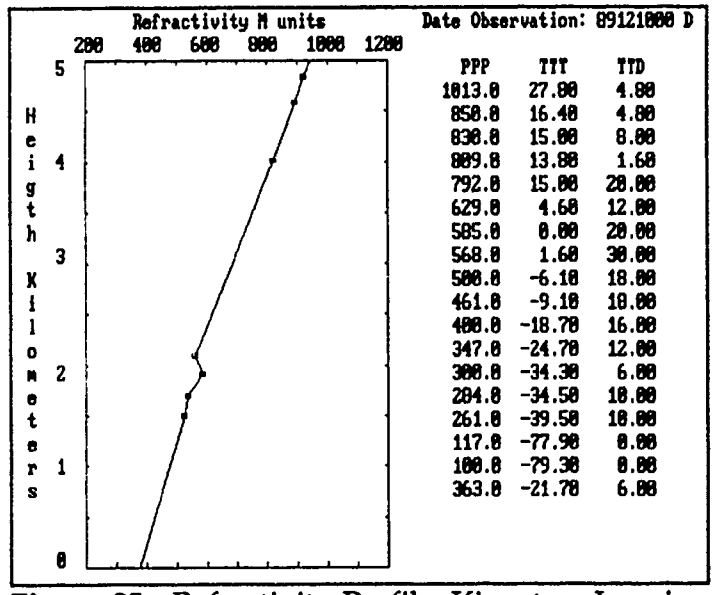

Figure 25. Refractivity Profile, Kingston, Jamaica, Station 78397, 10 Dec. 1989.

e. Roberts Field, Gran Cayman, Station 78384

For this station, 1148 soundings where processed and 381 soundings were found to contain trapping layers distributed as follows:

Year	1988	1989	Total
Soundings	618	530	1148
Surface based trapping layers	19	18	37
Elevated trapping layers (total)	194	150	344
Elevated trapping layers above 700 mb.	47	25	72
Total	213	168	381

The visual evaluation of the refractive profiles that contained trapping layers revealed that the elevated trapping layers where thick and strong and were grouped mainly near 1500 or near 3000 meters.

The occurrence of trapping layers was found to be 33.2 % and the occurrence of surface based trapping layers was 3.2 %.

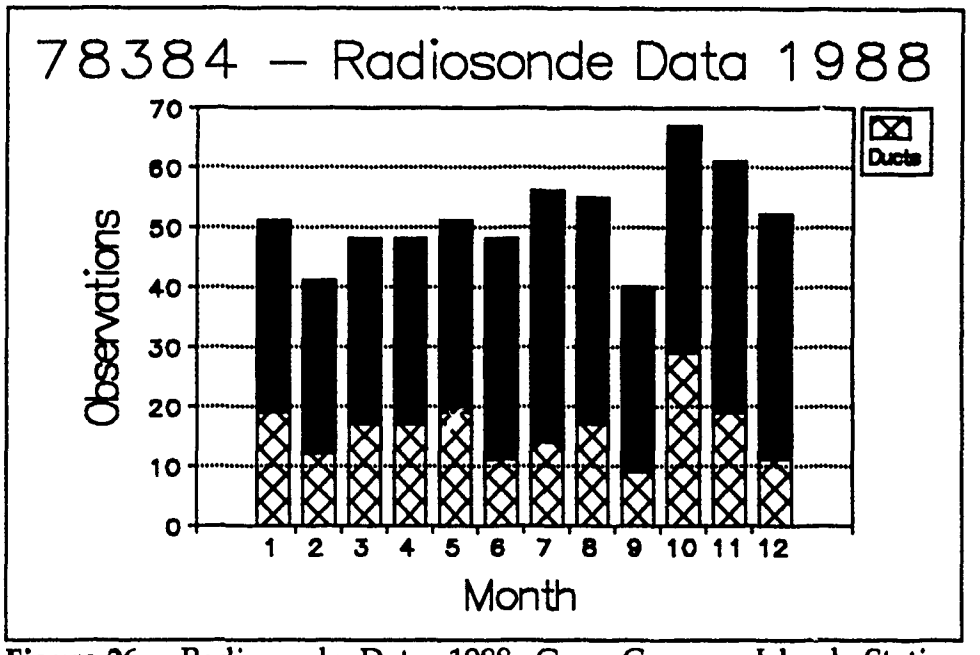

Figure 26. Radiosonde Data, 1988, Gran Cayman Island, Station 78384.

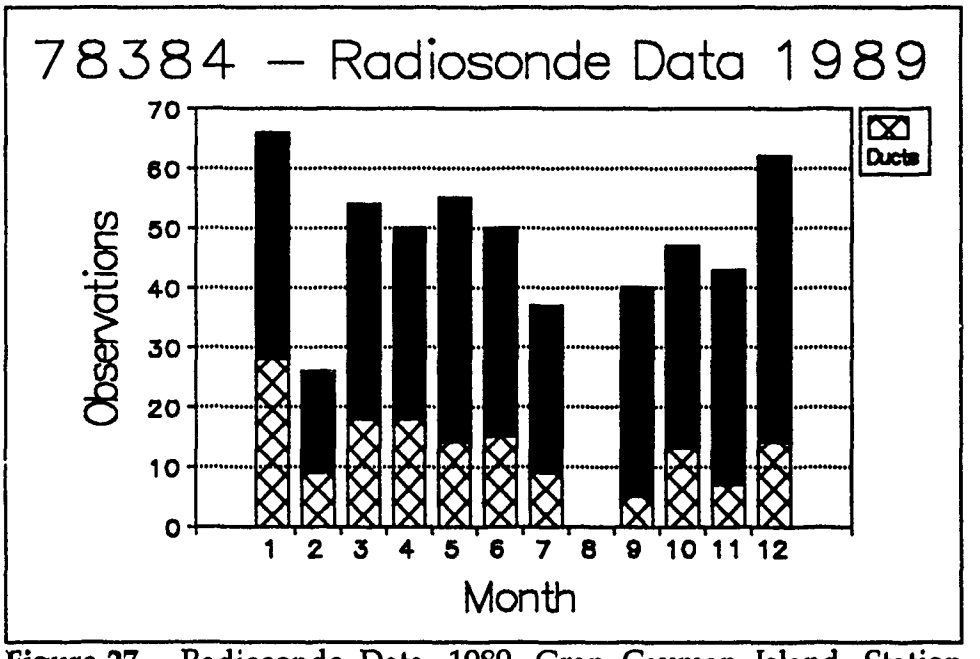

Figure 27. Radiosonde Data, 1989, Gran Cayman Island, Station 78384.

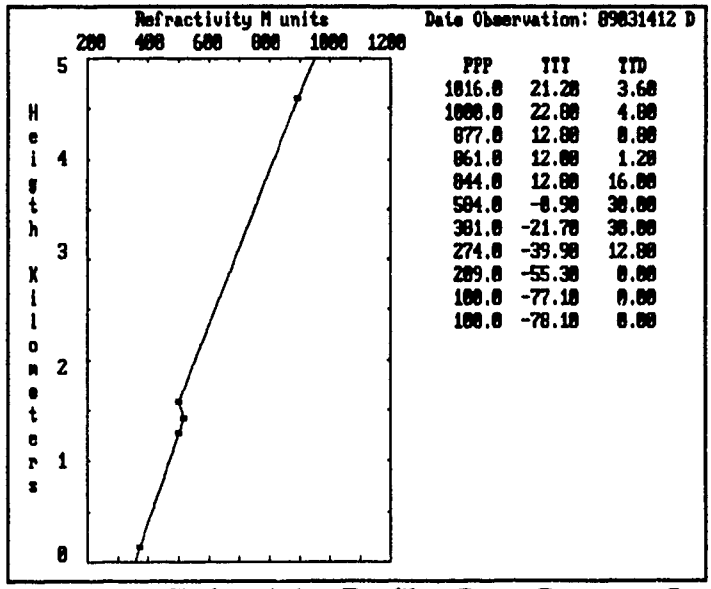

Figure 28. Refractivity Profile, Gran Cayman, Station 78384, 14 Mar. 1989.

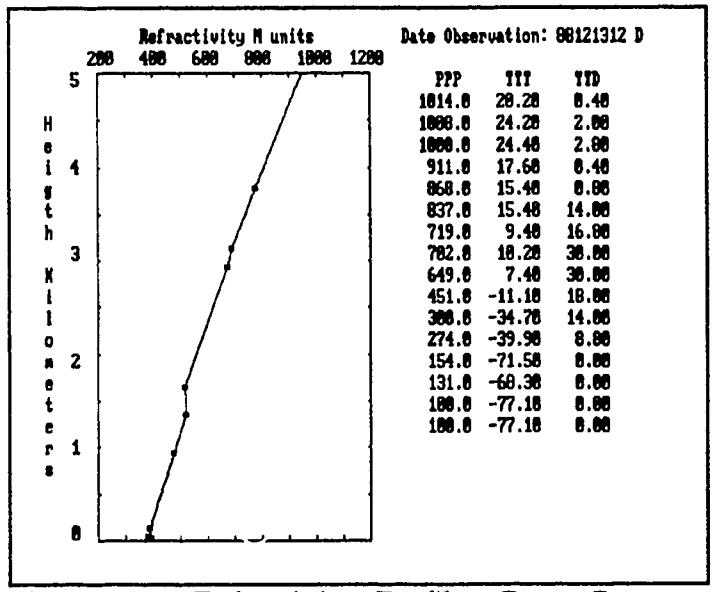

Figure 29. Refractivity Profile, Gran Cayman, Station 78384, 13 Dic. 1988.

V. PROPAGATION EFFECTS ON SYSTEMS

A. EFFECTS ON RADARS

The radar equation that conveniently describes the performance of a radar in terms of transmitted power, antenna gain and effective aperture, radar cross section of target and receiver sensitivity falls short when used to describe actual performance of systems.

> "In practice, however the simple radar equation does not predict the range performance of actual radar equipments to a satisfactory degree of accuracy. The predicted values of radar range are usually optimistic. In some cases the actual range might be only half that predicted." [Ref. 4]

The radar equation describes the free space range and assumes "...three-dimensionality and isotropy of space" [Ref. 1]. However, the atmosphere is in no way isotropic and the three-dimensionality is violated as soon as ducting or other anisotropic phenomena are encountered. Superrefraction and ducting can direct energy in a particular direction that otherwise would spread isotropically producing extended coverage, sometimes to ranges well beyond free-space ranges.

Extended range is not the only effect expected. Due to the reciprocal path, there is a significant increase in the clutter and noise received that can seriously degrade the overall performance of a surveillance system. Double return echoes are possible and a target at greater than the maximum

appear as an in-range target. The distance at which the signals can be intercepted will be augmented and the scenario becomes much more complex.

The surface-to-surface propagation over the ocean is affected in the area due to the moist MABL. The radio horizon (Page 10) is slightly extended on the mean over what would be expected over subtropical waters and somewhat larger than the world average.

1. Rain Effects

Rain is the most common and an important phenomena in tropical areas as nearly all tropical disturbances carry rain. Absorption and scattering of the radar energy by rain is a very strong loss mechanism. The difficulties involved in accurately measuring the characteristics and the rate of rainfall prevent the models from being effectively used to forecast the effect of rain on the radar coverage. MTI (Moving Target Indicator) or doppler radars show less rain clutter effects; but, since the energy is scattered in the rain volume, the effective power that reaches the target and the receiver is strongly reduced and, therefore, so is the detection range. The rain scatter is frequency dependent [Ref. 14] so low frequency radars can be used if see-through capability is needed.

The transient nature of rain, even in high precipitation areas like the Pacific ocean off the western coast of Colombia, suggest the selective use of sensors as the best way to obtain radar coverage during rain.

The transient nature of rain, even in high precipitation areas like the Pacific ocean off the western coast of Colombia, suggest the selective use of sensors as the best way to obtain radar coverage during rain.

2. Duct Effects

The range of radar coverage can be extended by surface based ducts associated with elevated trapping layers or by evaporation ducts. The evaporation duct is a subset of ducts where the duct base is at the surface. In the absence of a surface based duct, the evaporation duct is the dominant propagation mechanism for surface-to-surface detection over water, provided the radar antenna and the target are inside the duct and a frequency sufficiently high is used (above the cutoff frequency).

a. Coverage Diagram with Surface Based Duct

Due to the large number of different ducting profiles observed at the stations analyzed, the effects of a surface based duct on a particular system ducts will be illustrated using a sounding at station 80001 on March 14 1989. The refractive profile obtained from the sounding is depicted in Figure 13. A strong trapping layer is clearly visible from the surface up to 100 meters, causing a surface based duct. At around 3000 meters there is another thin duct. As stated earlier for this station, many soundings in which a duct is found revealed multiple ducts.

inside the duct. For comparison purposes, a standard refraction raytracing is shown in Figure 31.

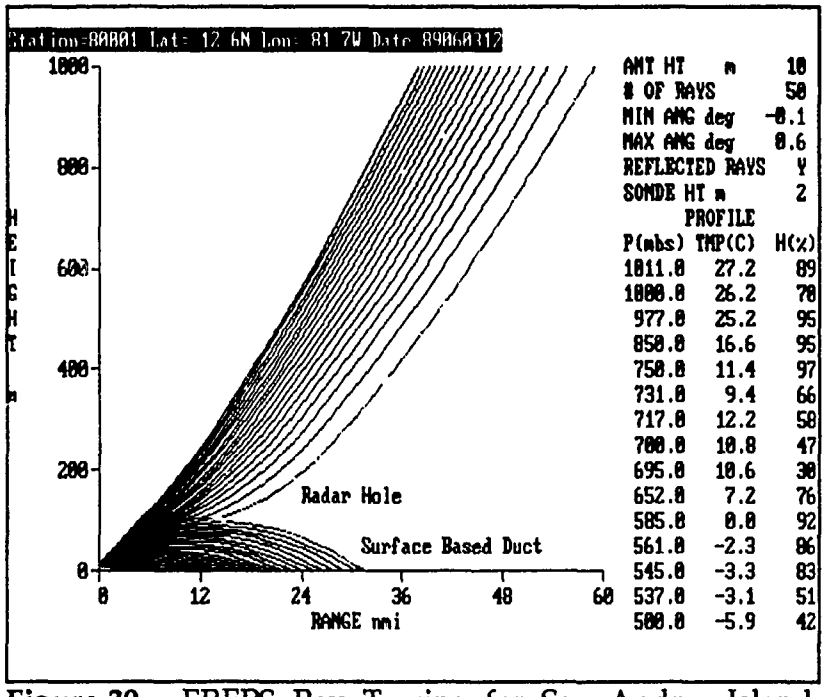

Figure 30. EREPS Ray Tracing for San Andres Island, Station 80001, 14 Mar. 1989.

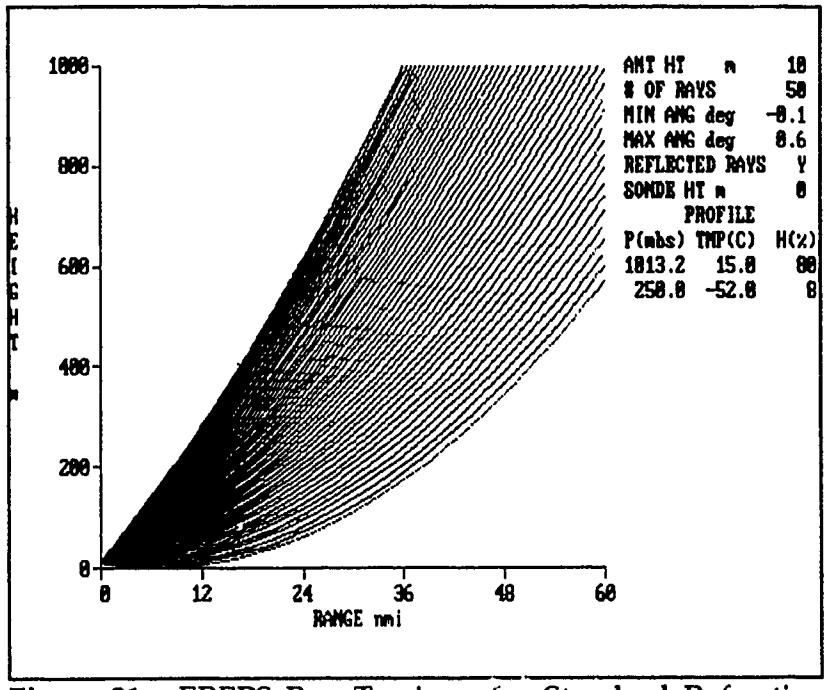

Figure 31. EREPS Ray Tracing of a Standard Refractive Atmosphere.

b. Propagation Loss

The ray tracing alone does not give enough information on the detection capability of a radar under specific refractive conditions. The system itself needs to be taken into account. Receiver characteristics as well as antenna gain, transmitter power, target size, thresholds and other factors need to be considered to assess detection capability. Table 3 lists the parameters necessary to estimate loss. The end application of the radar will ultimately dictate the probability of detection and false alarm rate to be included in the model.

Here, for the purpose of visualizing the effects of ducting in a given system, a "generic" surveillance radar is used with a target of small radar cross section

(RCS) and a Swerling model 1 [Ref. 4] to account for the slow fluctuation of RCS typical of a low tonnage vessel at sea.

Table 3

Parameters Used to Estimate Propagation Loss

Frequency	3 GHz.
Polarization	Horizontal
Radar height	10 meters
Target height	15 meters
Antenna type	Cosec-Sq.
Vertical BW.	10 degrees
Elevation Angle	0 degrees
Peak power	500 Kw.
Pulse width	1.0 uSec.
Antenna gain	32 dBi.
System losses	8.4 dB
Receiver noise figure	5 dB
Pulses integrated	10
RCS target	10 sqm.
Probability of detection	.8
Probability of false alarm	10^{-8}
Swerling case	1

The effects of the duct, shown in Figure 32, are tactically important. There is a significant skip zone in which there is no detection. The detection range is extended beyond the free-space range after the first reflection at 30 nm up to 55

nm. This an additional coverage of 6000 squared nautical miles to the 346 nm.[2] of the unextended coverage. If a force is aware of the presence of the duct, it can be used on purpose to get extended surface surveillance. Otherwise, the force can give away valuable intelligence by ignoring the existence of the duct.

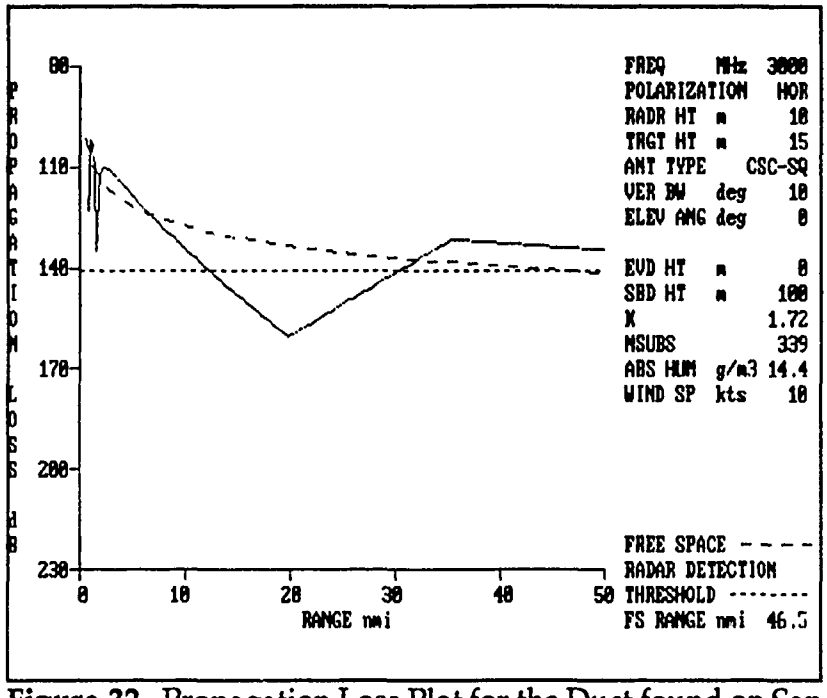

Figure 32. Propagation Loss Plot for the Duct found on San Andres Island, Station 80001 on 3 Jun. 1989.

The Evaporation duct exists nearly all the time. The summary data provided by EREPS calculated from 15 years of observations shows that an evaporation duct height of more than six meters 94.5 % of the time (Figure 33) and 16 or more meters high 53.1 % of the time. These are high values compared with the world

average (Figure 34). The evaporation duct is an important propagation mechanism, particularly for higher frequencies. Tactical effects of the evaporation ducts are often neglected and underestimated. Since the duct is present most of the time and is both frequency and height dependent, small vessels with their radar located inside the duct, operating in the X band, may have earlier detection of conventional platforms with higher antennas and lower frequency radars.

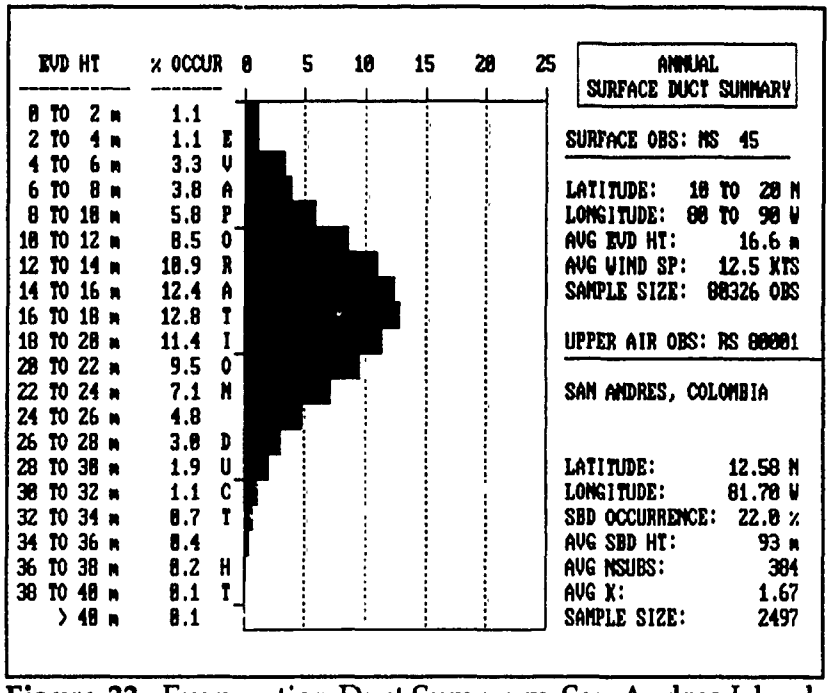

Figure 33. Evaporation Duct Summary, San Andres Island, Station 80001.

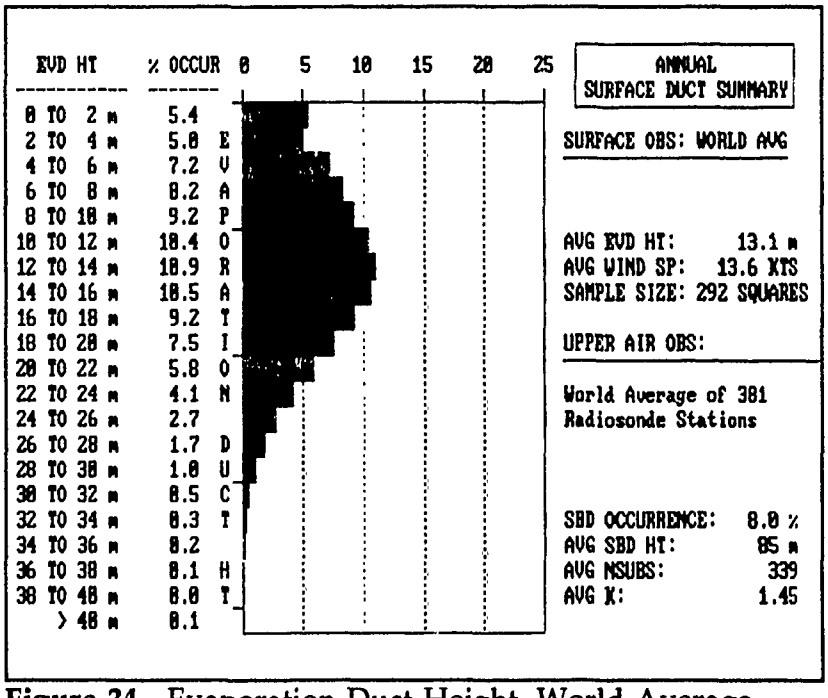

Figure 34. Evaporation Duct Height, World Average.

The range of the same radar in the presence of an evaporation duct of 16 meters is extended from 10 nmi. to 15 nmi., an increase in coverage from 314 square nmi to 706 square nmi. The increase in area coverage (225 %) and the relative permanence of the duct (expected 53% of the time at station 80001) make it an important propagation mechanism. The effects are shown in Figure 35.

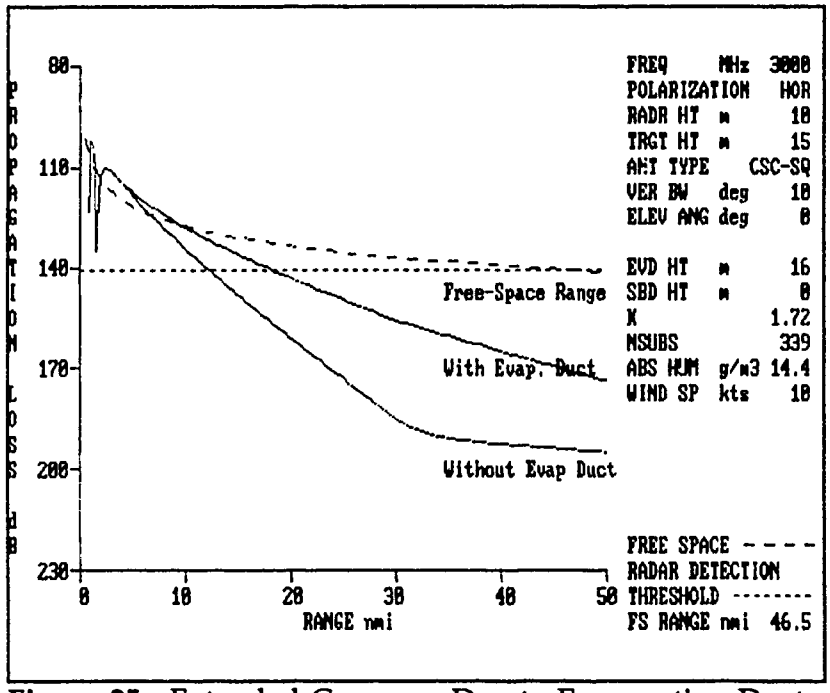

Figure 35. Extended Coverage Due to Evaporation Duct.

B. EFFECTS ON ESM

Anomalous propagation effects on ESM can be dramatic. Anomalous propagation can result in signal strength that are orders of magnitude bigger or smaller than the free-space signal, rendering relative signal strengths useless

as a rough distance measure; and the attenuation effects are not readily observed in the displays due to the passive nature of the system.

Today's expected operating environment is so dense that digital processing techniques are always used in conjunction with ESM and radar warning receivers (RWR) to sort and extract the various parameters of a signal. Sensitive ESM receivers suitable for electronic intelligence gathering (ELINT) will eventually operate in such a high densities that the processing cannot cope with the task. The probability of intercept for a given signal will be greatly reduced.

The saturation of the processing can result from any mechanism that effectively brings more signals into the receiver. Altitude, in an airborne receiver, and ducts, for both surface and air borne systems, effectively extend the radius of coverage for a given sensitivity. Assuming a given number of emitters per unit area, the number of emitters received will follow the square of the range covered, resulting in a substantial increase of the density of the environment. What could be seen as an advantage of getting extended coverage can very well result in a lower probability of intercept for all signals.

VI. CONCLUSIONS

The atmospheric effects on VHF/UHF/Microwave propagation in the tropical waters surrounding Central America are significant. There is a high probability of ducting and extended radar horizon is expected most of the time.

Statistical and historical data are based on the soundings taken by the WMO station network. These soundings are used for the synoptic scale weather analysis and are not intended for local refractivity study. Data collection is seriously flawed when the times, instruments and collection procedures are not precise and consistent enough to draw conclusions on the more dynamic refractivity behavior. There is no substitute for real time, tactically planned soundings and data collection.

The data available for the area are therefore just a sample taken at the few stations shown and at particular times in which ducting is more probable. The analysis of the results of refractivity studies using these data should be done using extreme caution. The overall tropical environment must be evaluated for consistency. Routine software checks are not enough when dealing with atmospheric data. Knowledge of the physics involved in the atmospheric behavior is necessary for military personnel due to the operational consequences of incorrectly assessing refractive conditions.

Further studies are needed to validate the interpretation of the refractive data available for the area against measurements or case observations. There are few seasonal variations in the temperature and wind in the tropical area and therefore correlation with satellite imagery may be useful in determining the extent of anomalous refractive conditions.

There is the need for increasing the awareness of the military on the effects of propagation on the systems and tactics to be used, as well as the particular climatology of the operating theater in Central America. The study of the environment and its effects on radio propagation should be included in the undergraduate education and intensified in the graduate education to provide a wide base of knowledge and understanding of systems capabilities.

The only radiosonde data available for the Pacific Ocean comes from the Howard Air Force Base, Panama Canal Zone, which, as seen in the map in Figure 8, cannot be very representative of the conditions in Central America's Pacific Ocean area. Not enough data is available to even characterize the refractive phenomena that may occur there. Alternative sources such as satellite imagery and remote sensing of the atmosphere could be used to obtain the data that current environmental models use.

APPENDIX A.

The programs to manipulate the radiosonde data were written in Quick-Basic(R) version 4.5 and are too big to list, the routines used to obtain modified refractivity and height and the general subprogram used to identify and plot ducts, are presented here.

```
  ' P          Pressure in millibar
  ' Ta         Temperature in Kelvin
  ' e          Partial pressure of water vapor in millibar
  ' H          Height in meters
  '
    FUNCTION RefractM (p, Ta, e, H)

          M = 77.6 * p / Ta + 3.73 * 10 ^ 5 * e / (Ta * Ta)
+ H / 6.371
          RefractM = M

    END FUNCTION



  ' Function to find the saturated vapor pressure (millibar)
  ' using Lowe's polynomial
  ' Temperatures in Celsius
  '
    FUNCTION Satvp (Temp)

        DEFDBL A

        A0 = 6.107799961#
        A1 = .4436518521#
        A2 = .01428945805#
        A3 = .0002650648471#
        A4 = .000003031240396#
```

```
        A5 = 2.0340809481D-08
        A6 = 6.136820928999999D-11

        Svp = (((Temp * A6) + A5) * Temp + A4)
        Svp = ((Svp * Temp + A3) * Temp + A2) * Temp + A1
        Svp = Svp * Temp + A0
        Satvp = Svp

    END FUNCTION




' H0    Initial Height, meters
' Vt0   Virtual Temperature at Initial Height, Kelvin
' P0    Pressure at Initial Height , mbar
' Vt1   Virtual Temperature at Actual Height, Kelvin
' P1    Pressure at Actual Height , mbar
'
    FUNCTION Height (H0, Vt0, Vt1, P0, P1)
          Height = H0 + 14.63 * (Vt0 + Vt1) * LOG(P0 / P1)
    END FUNCTION



' Ta  Absolute temperature (Kelvin)
' P1  Pressure
' Ee  Vapor pressure environ.
'
     FUNCTION Tv (Ta, P1, Ee)

          Tv = Ta + (.3794017# * Ta * Ee) / (P1 - Ee)

     END FUNCTION



'
SUB Process (Alt$, Layer$, Intensity, DuctHeight, NrData%)
        Layer$ = " "
```

```
Tmp$ = ""
Intensity = 0
LayerHeight = 0
P0 = ppp(0)
H0 = VAL(Alt$)
H(0) = H0

FOR i = 0 TO NrData% - 1
    Td = TTT(i) - TTD(i)
    Ee = Satvp(Td)
    Ta = AbsoluteTemp(TTT(i))
    P1 = ppp(i)
    Vt1 = Tv(Ta, P1, Ee)
    IF i = 1 THEN
        Vt0 = Vt1
    END IF
    H(i) = Height(H0, Vt0, Vt1, P0, P1)
    M(i) = RefractM(P1, Ta, Ee, H(i))
    H0 = H(i)
    P0 = P1
    Vt0 = Vt1

    IF H(i + 1) - H(i) = 0 THEN
        Duct$ = "X"
        dMdZ(i) = 0
        GOTO OnZero
    END IF
    dMdZ(i) = (M(i + 1) - M(i)) / (H(i + 1) - H(i))
    OnZero:
    IF dMdZ(i) < 0 THEN
        SELECT CASE ppp(i)
        CASE IS > 700
            Layer$ = "D"
            LayerHeight = H(i)
            IF i = 0 THEN
                Layer$ = "S"
            END IF
        CASE IS < 700
            IF Layer$ = " " THEN
                Layer$ = "d"
                LayerHeight = H(i)
            END IF
```

```
            END SELECT
        END IF
        IF dMdZ(i) < Intensity THEN
            Intensity = dMdZ(i)
        END IF
    NEXT i

    'Plot the Layers found below 700 mbars.

    IF Layer$ = "D" OR Layer$ = "S" THEN
        Plot M(), H(), NrData%, Layer$
    END IF

END SUB
```

LIST OF REFERENCES

1. Blake, L.V., 1980: *Radar Range-Performance Analysis*, LexintonBooks.

2. M.Neiburguer, J.G.Edinger and W.D.Bonner, *Understanding Our Atmospheric Environment*, W.H.Freeman and Co., San Francisco.

3. W.,J.,Shaw, *Meteorology For EW, Class Notes*, 1988.

4. Skolnik M. I. 1980, *Introduction to Radar Systems*, McGraw-Hill.

5. Jordan, C.,L., 1958: Mean Soundings for the West Indies area, *Journal of Meteorology*, Vol. 15, p.91-97.

6. Paulus,R.A. *Specification for Evaporation Duct Height Calculations*, Technical Document 1596, Naval Ocean Systems Center, 1989.

7. F.R.Williams and others,*Forecasters Handbook for Central America and Adjacent Waters*, Technical Report TR 89-08, Naval Environmental Prediction Research Facility, 1989.

8. USAF Environmental Technical Applications Center, TN-89/003,*The Caribbean Basin - A Climatological Study*, K.R.Walters, A.G.Korik and M.J.Vojtesak, 1989.

9. *Basic Synoptic Networks of Observing Stations*, WMO Secretariat, Geneva Switzerland, 1981.

10. Patterson,W.,L., and others, *Engineer's Refractive Effects Prediction System (EREPS) Revision 2.0*, Technical Document 1342, Naval Ocean Systems Center, 1990.

11. P.R.,Lowe, "An Approximating Polynomial for the Computation of the Saturation vapor Pressure", *Journal of Applied Meteorology*, 1977, Vol. 16, p:100-103.

12. Hess,S.L. *Introduction to Theoretical Meteorology*, Holt, Rinehart and Wiston, New York, 1959.

13. L.N. Ortenburguer, and S.B.Lawson, *Radiosonde Data Analysis IV*, GTE Government Systems Division, 1985.

14. Eaves, J.L., 1987, *Principles of Modern Radar*, Van Nostrand Reinhold Company, New York.

INITIAL DISTRIBUTION LIST

		No. Copies
1	Defense Technical Information Center Cameron Station Alexandria, VA 22304-6145	2
2	Library, Code 52 Naval Postgraduate School Monterey, CA 93943-5000	2
3	Professor K.L. Davidson, Code MR/DS Naval Postgraduate School Monterey, CA 93943-5100	5
4	Professor F.R. Williams, Code MR/WF Naval Postgraduate School Monterey, CA 93943-5100	1
5	Roger Helvey Geophysics Division Pacific Missile Test Center Point Mugu, CA 93042	1
6	Sr. Almirante Comandante Armada Nacional Comando Armada Nacional C.A.N., Avenida El Dorado Bogotá D.E. Colombia	3
7	Sr. Contralmirante Director Escuela Naval Almirante Padilla Escuela Naval, Manzanillo Cartagena, Colombia	2
8	Sr Contralmirante Agregado Naval Embassy of Colombia Office of the Naval Attache 2118 Leroy Place Washington D.C. 20008	1

9	Sr. Capitan de Fragata Director C.I.O.H. Escuela Naval, Manzanillo Cartagena, Colombia	1
10	Teniente de Navío Mauricio Gaviria Maldonado. Apartado Aereo # 20152 Cartagena, Colombia	2